

ADA1031,05

12 LEVEL II

Technical Note

TN no. N-1595



title: PROPELLANT-EMBEDDED ANCHORS:
PREDICTION OF HOLDING CAPACITY IN
CORAL AND ROCK SEAFLOORS

author: J. F. Wadsworth, III and R. M. Beard

date: November 1980

DTIC
ELECTE
S D
AUG 20 1981
B

sponsor: Naval Facilities Engineering Command

program nos: YF59.556.091.01.204



CIVIL ENGINEERING LABORATORY

NAVAL CONSTRUCTION BATTALION CENTER
Port Hueneme, California 93043

Approved for public release; distribution unlimited.

81 8 19 072

FILE COPY

Unclassified

SECURITY CLASSIFICATION OF THIS PAGE (When Data Entered)

REPORT DOCUMENTATION PAGE		READ INSTRUCTIONS BEFORE COMPLETING FORM
1. REPORT NUMBER TN-1595	2. GOVT ACCESSION NO. DN987005	3. RECIPIENT'S CATALOG NUMBER AD-A103-105
4. TITLE (and Subtitle) PROPELLANT-EMBEDDED ANCHORS: PREDICTION OF HOLDING CAPACITY IN CORAL AND ROCK SEAFLOORS		5. TYPE OF REPORT & PERIOD COVERED Not final; Oct 1977 - Sep 1979
6. AUTHOR(s) J. F. Wadsworth, III and R. M. Beard		6. PERFORMING ORG. REPORT NUMBER
9. PERFORMING ORGANIZATION NAME AND ADDRESS CIVIL ENGINEERING LABORATORY Naval Construction Battalion Center Port Hueneme, California 93043		10. PROGRAM ELEMENT, PROJECT, TASK AREA & WORK UNIT NUMBERS 62759N; YF59.556.091.01.204
11. CONTROLLING OFFICE NAME AND ADDRESS Naval Facilities Engineering Command Alexandria, Virginia 22332		12. REPORT DATE November 1980
14. MONITORING AGENCY NAME & ADDRESS (if different from Controlling Office)		13. NUMBER OF PAGES 70
		15. SECURITY CLASS (of this report) Unclassified
		16. DECLASSIFICATION/DOWNGRADING SCHEDULE
16. DISTRIBUTION STATEMENT (of this Report) Approved for public release; distribution unlimited.		
17. DISTRIBUTION STATEMENT (of the abstract entered in Block 20, if different from Report)		
18. SUPPLEMENTARY NOTES		
19. KEY WORDS (Continue on reverse side if necessary and identify by block number) Plate anchors, propellant-embedded anchors, anchors, seafloors, moorings, coral seafloors, rock seafloors.		
20. ABSTRACT (Continue on reverse side if necessary and identify by block number) Propellant-embedded anchors have become an important asset in the Navy's mooring equipment inventory. They offer potential for anchoring in coral and rock seafloors where conventional anchors will not work or present logistic problems. Most operational installations of propellant-embedded anchors have been in coral seafloors and these anchors have usually been proof-loaded to their design capacity. The ultimate capacities of these		

(continued)

DD FORM 1 JAN 73 1473 EDITION OF 1 NOV 65 IS OBSOLETE

Unclassified

SECURITY CLASSIFICATION OF THIS PAGE (When Data Entered)

Unclassified

SECURITY CLASSIFICATION OF THIS PAGE When Data Entered:

20. Continued

installations have not been determined, hence the full potential of propellant-embedded anchors in coral has not been determined. This report presents the results of a program of model and full-scale propellant-embedded anchor tests in coral and rock. The significance of the results and analysis of the data are presented. A promising equation for predicting holding capacity in coral is developed from the data. It is concluded that the data base of tests in rock is not sufficient for developing an equation for prediction of holding capacity.

Library Card

Civil Engineering Laboratory
PROPELLANT-EMBEDDED ANCHORS: PREDICTION OF
HOLDING CAPACITY IN CORAL AND ROCK SEAFLOORS,
by J. F. Wadsworth, III and R. M. Beard
TN-1595 70 pp illus November 1980 Unclassified

1. Propellant-embedded anchors 2. Moorings I. YF59.556.091.01.204

Propellant-embedded anchors have become an important asset in the Navy's mooring equipment inventory. They offer potential for anchoring in coral and rock seafloors where conventional anchors will not work or present logistic problems. Most operational installations of propellant-embedded anchors have been in coral seafloors and these anchors have usually been proof-loaded to their design capacity. The ultimate capacities of these installations have not been determined, hence the full potential of propellant-embedded anchors in coral has not been determined. This report presents the results of a program of model and full-scale propellant-embedded anchor tests in coral and rock. The significance of the results and analysis of the data are presented. A promising equation for predicting holding capacity in coral is developed from the data. It is concluded that the data base of tests in rock is not sufficient for developing an equation for prediction of holding capacity.

Unclassified

SECURITY CLASSIFICATION OF THIS PAGE When Data Entered:

CONTENTS

	Page
INTRODUCTION	1
CORAL ANCHORS	1
Previous Tests	2
Barbers Point Tests	2
BARSTUR Tests	3
Analysis of Test Data	4
Prediction of Holding Capacity	4
ROCK ANCHORS	6
Previous Tests	6
NWC, China Lake Tests	7
Analysis of NWC Test Data	7
White Sands Missile Range Tests	8
Analysis of White Sands Missile Range Data	9
Development of Empirical Holding Capacity Equation for Rock Seafloors	10
SUMMARY	14
CONCLUSIONS	14
RECOMMENDATIONS	15
REFERENCES	16

INTRODUCTION

The Civil Engineering Laboratory has developed propellant-embedded anchors as an alternative anchoring system. These anchors can be used in situations where conventional anchors are difficult to use or will not meet mooring design requirements. In the early stages, the anchors were developed for use by Navy salvage vessels in coral seafloors (NAVSHIPS 0994-002-6010; Smith, 1971). Since that time embedment anchors of varying designs and sizes have been tested and used in a variety of seafloors (Taylor, 1976; True and Taylor, 1976; True, 1977; Wadsworth and Taylor, 1976). Propellant-embedded anchors are being used because they are easy to precisely install with no chance of the anchor dragging out of position.

Of the anchors that have been installed for actual operational use, most have been in coral seafloors. These installations have usually been proof loaded to design capacity; however, few data on the ultimate holding capacities of the anchors have been acquired. Consequently, it is not known at what factor of safety these anchorages have been used. The factor of safety may have been small or quite large.

There has been no operational use of the propellant-embedded anchors in rock. An attempt to place a mooring for a semi-submersible drilling rig in rock using a coral type projectile was not successful. Several rock flukes for propellant-embedded anchors have been built and tested with sharply inconsistent results. If the performance of rock flukes could be made more consistent and predictable, it is likely they would be widely used because of their high efficiency and because mooring scopes could be reduced (Valent, 1973 and Wadsworth, 1976).

This report presents the results of a program of model and full-scale embedment anchor tests in coral and rock. The significance of the tests is discussed, and analyses of the test data are presented. Based on the test data, separate equations are developed for predicting holding capacity in coral and rock seafloors. This work was sponsored by the Naval Facilities Engineering Command and funded under the Ocean Facilities Engineering Program.

CORAL ANCHORS

The configuration of the coral flukes has undergone many changes during the development of the various embedment anchors (Figures 1 through 6). The present coral fluke design is basically the same for each of the CEL anchors. The only difference is that the 20K and 10K coral flukes (Figures 5 and 6) have a spur on the bottom of the fluke. This spur was added to induce a keying action in soft coral seafloors. It also balances the mass of the projectile so the main fluke plate is close to the axis of the piston. The spur is not necessary on the larger 100K anchor.

Previous Tests

Embedment anchors have been tested by both the Navy and the Army. Results of tests conducted in coral seafloors prior to this project are listed in Table 1. Most of these tests were of limited use in a data base because of the variation in fluke configurations and the lack of data on properties of the seafloor materials. Samples of coral from around the embedded flukes were collected by divers in two of the test series: the SUPSLAV anchor tests at Barbers Point, and the CEL 20K anchor installations for the Barking Sands Underwater Range Extension (BSURE) mooring. Diego Garcia and Argus Island are mooring and salvage reaction point installations in coral with the CEL salvage and 100K anchors, respectively. In these cases, no attempts were made to pull out the flukes, but proof-loads were applied, and these proof-load data mark a lower bound holding capacity. Review of the available data indicated additional coral tests were required to develop a method to predict holding capacities in coral seafloors.

Barbers Point Tests

Barbers Point, Oahu was selected as the site for full-scale tests in coral. Testing at this site offered three advantages: (1) some knowledge of the seafloor properties already existed from the SUPSLAV tests, (2) a direct comparison to previously acquired data would be possible, and (3) support was available at nearby Pearl Harbor. In order to conduct as many tests as possible with the available resources, a lightweight propellant-embedded anchor (CEL 10K anchor, Figure 7) was chosen.

The Barbers Point tests were conducted in June 1978. Harbor Clearance Unit One provided the supporting personnel and equipment to install the anchors. The craft used was a LWT, an aluminum side-loadable warping tug. The anchors were raised and lowered using a bow A-frame and a 3-ton-rated pneumatic winch. After installation of each anchor, the winch was used to its capacity to proof load the embedded fluke.

All 12 anchors to be tested were installed in 1 day. The embedded flukes were then surveyed by an engineer-diver. Figure 8 is a photograph of a typical embedded fluke. Four of the flukes were embedded in coral beneath a sand layer and could not be inspected. Each site was photographed, fluke penetration and size of impact crater measured, site markers placed, and samples of loose coral collected from around the fluke.

The anchors were load tested by the USS BEAUFORT ATS-2. Loads were applied by connecting into the anchor downhaul with a wire rope led over a bow roller, taking out the slack with the capstan, placing the line in a carpenter stop, then applying load by backing down the ship. Loads were measured using an in-line load cell. Eight of the 12 anchors failed when the wire rope downhaul failed; only four flukes were extracted. Following the load tests the anchor sites were again inspected by divers. Figure 9 is a photograph of the same fluke shown in Figure 8 after loading. Note that there is no evidence of the fluke extracting or of the surrounding coral displacing; this was typical of the flukes that

could be inspected. Figure 10 is a before and after photograph of one of the flukes which did extract. Complete information on the results of the load tests is given in Table 2.

Review of the test results and procedures indicates that the recorded loads may have been considerably lower than the loads actually applied at the anchors. First, the load line to the anchors passed over the ship's bow roller. Friction and the inertia of this roller would result in different line tensions inboard and outboard of the roller. Second, the swell and sea under which the tests were conducted resulted in very rapid load applications (snap loads) that probably exceeded the load recorder's dynamic response capability. Third, one anchor that had been proof loaded to a nominal 26 kN from the installation craft was pulled out by the BEAUFORT at a measured load of only 4.5 kN. Fourth, eight of the 12 tests ended when either downhaul cables or mechanical connections at the fluke failed. All of these failures occurred at on-deck recorded loads much lower than the breaking strength of the failed mechanical parts (~260 kN).

BARSTUR Tests

The 20K coral embedment anchors that were installed off Nohili Point at the Barking Sands Tactical Underwater Range (BARSTUR) in August 1976 (see data in Table 1) provided an opportunity to conduct pull tests on previously installed anchors. The anchors had been used to moor a cable-laying ship during installation of the shore end of the cable runs coming in from the new, expanded range. Figure 11 is a sketch of the design of each mooring leg. Note that two 20K anchors were used for each mooring leg. Following this use, the buoys were removed from three of the five moorings, and the wire rope bridles and downhauls were laid on the bottom. The other two moorings were used to moor two large navigational buoys.

CEL requested and received permission from the Pacific Missile Test Center (PMTC) to perform pull tests on the six unused anchors. Since a detachment from Underwater Construction Team Two (UCT 2) was to perform a cable survey at BARSTUR in the summer of 1978, PMTC also granted CEL the use of the detachment to locate and buoy the anchors to be tested. A section of the bridle, the wire rope connecting two anchors at each mooring, was recovered and returned to CEL for testing. The downhauls and bridles had been submerged for 2 years with no corrosion protection, but the two sections tested broke at 329.3 kN and 258.1 kN. The rated breaking strength for this 7/8-inch-diameter 6x19 wire rope was 354.2 kN. The wire ropes, thus, seemed to be in satisfactory condition to place meaningful loads on the anchors (the original mooring design had assumed each anchor to hold 222.5 kN).

Load tests were performed with the USS BRUNSWICK (ATS-3) in the same manner as was used earlier at Barbers Point. A strap of nylon line was added to the load line to reduce the snap loads experienced at Barbers Point. Also, sea conditions were better, which allowed a more gradual loading. The anchors were surveyed before and after load testing, with the test results as shown in Table 3. In every case the wire rope downhaul failed, thereby establishing a lower bound holding capacity. Note that the failure loads are below the breaking loads of two test

sections of wire rope. It is thought the reasons for this are similar to those for a similar problem with the Barber's Point tests. Post-test diver surveys failed to show any displacement of the anchor or the surrounding coral.

Analysis of Test Data

The data from the Barbers Point 10K anchor tests, the BARSTUR 20K anchor tests, and the proof loading data for the 100K anchor from Diego Garcia and Argus Island were plotted as histograms with the normal curve added. Figures 12, 13, and 14 show these data. The 90% confidence limit, the holding capacity which will be exceeded 90% of the time, is plotted for each case. The confidence of exceeding the rated holding capacity is 95% for the 10K anchor, greater than 99% for the 20K anchor, and 88% for the 100K anchor.

The confidence limits and mean holding capacities given in the figures are conservative since only 3 of the 11 data points in the 10K test data and none of the 20K or 100K test data are actual anchor extractions. The data are either the maximum proof-load applied or the maximum recorded loads experienced before the wire rope downhaul failed. Actual anchor pullout loads would shift the curves in Figures 12, 13, and 14 further to the right than is shown. In addition, the wire rope failures at Barbers Point and BARSTUR were recorded at levels much less than the rated breaking strength. It is likely that much higher loads occurred but were not recorded on deck due to friction and inertia of the ATS bow sheave or a slow response from the load recorder.

Prediction of Holding Capacity

Data Base. An equation for predicting holding capacity in coral seafloors can be developed from test data only where the anchor flukes were pulled out. This places a restriction on the data base because it eliminates data from both proof-loading tests and tests that resulted in mechanical failure of anchor hardware. Table 4 lists all the data found on embedded anchor coral tests listed in Table 1. Where known, the values of parameters that are thought to have the most influence on holding capacity are listed in Table 4 for each test. The fluke mass (m) and velocity (v) provide a measure of the energy available for penetration. Fluke frontal area (F) affects penetration while the fluke's embedded surface area (A) determines the area over which the fluke and coral interact to provide holding capacity. Fluke load point eccentricity, e , and loading angle, θ , define nonfrictional aspects of holding capacity. Load point eccentricity is defined as the ratio of eccentricity of the downhaul attachment point from the main fluke axis to the length of the fluke. Two coral properties, unconfined compressive strength (σ) and the dry unit weight (ρ), help to define the effect of the target material. Also included are the data from two model coral fluke tests performed at NWC, China Lake, in a chalky limestone that simulated a soft coral. Nineteen of these tests resulted in pullout of an anchor fluke and are listed separately in Table 5.

There are two major problems with this data base. First, an examination of Table 5 shows that in many cases parameters are unknown. Of particular concern is the absence of coral properties for the first 14

tests listed. Second, the load measurements for the three CEL 10K anchor tests at Barber's Point are not thought to be indicative of the loads applied to the flukes as previously discussed. These 17 tests cannot, therefore, be used to determine the relative significance of the various parameters affecting holding capacity. There are then only two tests, the model 20K tests at China Lake, that are usable for developing a predictive equation that is a function of fluke and coral parameters. However, this data base is too narrow to achieve a meaningful result.

Development of Empirical Holding Capacity Equation. In spite of the difficulties with the data, an effort was made to determine the relative significance of the parameters. This was done by performing linear regression analyses for different combinations of test parameters using a method described by Tolson (1970). No distinction was made between proof loads, pullout loads, or loads that caused hardware failures. The dominating parameters were found to be fluke mass and velocity. Some coral property, however, seems to be a necessary ingredient as it affects both penetration and pull resistance.

An equation was then developed for holding capacity, H , as a function of fluke mass, m , fluke velocity, v , and coral compressive strength, σ .

$$H = f(m, v, \sigma) \quad (1)$$

From dimensional analysis it can be shown that

$$H^3 = f(\sigma \cdot m^2 \cdot v^4) \quad (2)$$

or

$$H = k \cdot \sigma^{1/3} \frac{1}{2} m v^{2/3} \quad (3)$$

Equation 3 is dimensionally correct and shows that holding capacity should be strongly influenced by the kinetic energy ($KE = 1/2 mv^2$) of the fluke and only moderately influenced by the coral's compressive strength (since H varies as the cube root of σ).

It is not possible to test this equation against the data base because of the paucity of information on coral strength for the tests where anchors pulled out. However, because coral strength is not nearly as significant a parameter as kinetic energy, a plot was made of holding capacity versus just kinetic energy (Figure 15). Every test from Table 4, where the kinetic energy could be determined and the holding capacity was known (58 data points), is included except for the fifth CEL 10K anchor test at Barber's Point. This test was excluded because the load measurement was very inaccurate. The circled points in Figure 15 represent tests where pullout was achieved. The best fit equation for all the data is:

$$H = 0.068 KE^{0.58} \quad (4)$$

The best fit equation for the data points where pullout occurred is:

$$H = 0.024 KE^{0.684} \quad (5)$$

Both equations are made dimensionally correct by making the units of the constants the cube root of N/m^2 when the kinetic energy is in joules. Single-sided lower bound 90% confidence limits are presented in Figure 15 along with each best fit line. What is very significant about both of these equations, and particularly Equation 5, is that the power of the kinetic energy term is very near the two-thirds power derived by dimensional analysis. This result also suggests that Equation 3 may be an appropriate equation for including coral properties. However, the determination of the empirical constant for Equation 3 requires additional data not presently available.

Equation 4 is more a summary of experience with various coral anchors than a predictor of holding capacity. This is because three-fourths of the data upon which it is based are proof loads and hardware failures. It provides a very conservative estimate of holding capacity. On the other hand, Equation 5 is based only on pullout data and does provide a true estimate of ultimate holding capacity. On Figure 15, lines have been marked at the kinetic energies of the four CEL propellant-embedded anchors at optimum ballistic performance with a coral fluke. Table 6 is a tabulation of the predicted mean holding capacities and the holding capacities expected to be exceeded 90% of the time for each of the anchors.

There are limitations to Equation 5. Because it does not take into consideration coral properties or fluke shape, its use is restricted to the fluke shape and range of properties given in Table 5. However, as shown by Equation 5 and as discussed by Taylor (1976) for sediments, the holding capacity of a given propellant-embedded anchor is largely a function of the energy transferred to the fluke. Therefore, Equation 5 should have considerable usefulness in predicting the holding capacity in coral of the CEL propellant-embedded anchors.

ROCK ANCHORS

Previous Tests

The amount of existing data on propellant-embedded anchors in rock is considerably less than the data available for coral. The fluke designs which have been used have had mixed success (Smith, 1971; Taylor and Beard, 1973; Taylor, 1976). The SUPSALV rock fluke (Figure 16) was simply a coral projectile modified by increasing the fin's taper and hardening the projectile tip. The CEL 20K rock fluke design (Figure 17) was based upon the SUPSALV anchor results, the scale model tests conducted in a simulated rock medium (True, 1975), and the rock penetration work conducted by Sandia Laboratories (Young, 1970).

After testing of these flukes recommendations were made by the investigators to conduct further research and development on a rock fluke for embedment anchors. Following preliminary assessments (Wadsworth, 1976; Beard and Wadsworth, 1976) it was decided that the best approach

to developing an understanding of embedment anchor holding capacity in rock was to perform as many large-scale model tests as possible in a variety of rock types.

NWC, China Lake Tests

The first series of tests was conducted to explore the effect of different projectile shapes and ballistic parameters upon holding capacity. The tests were conducted in exposed outcrops of granite and extrusive basalt at the Naval Weapons Station, China Lake, Calif. Tests were conducted on land to allow a greater number of tests to be conducted with available funds. The anchor projectiles were launched by the Magnavox Company's propellant-embedded anchor test stand which was developed for firing the 7-pound Magnavox propellant-embedded anchor flukes on land. The propellant energy is transferred to the flukes by a piston that mates to the fluke and is inserted into the gun barrel. Using this launcher, a 1:3.75 geometric scale could be used assuming the 20K anchor as the prototype. Impact velocity of these models was the same as that of the prototype.

Eight different fluke shapes were used in these experiments. They are designated as Dart, Serrated Dart, Star, Cone, Stake, Serrated Stake, Tapered Stake, and Coral and are depicted in Figure 18. The Dart was considered to be the control fluke as it was geometrically scaled down from the 20K anchor rock fluke then in use. The Serrated Dart and Star are variations of this shape. The three stake shapes represent a significant departure from the DART as does the CONE. Each of the STAKE projectiles was shortened to keep the L/D ratio below 8. The weight lost by removing the fins and shortening the body was made up by using a heavier piston. The Coral was a scaled down coral fluke.

These shapes were all tested in a weathered granite and, with the exception of the coral fluke, in basalt as well. Only the coral fluke was tested in a chalky limestone, and those results are given in the section on coral anchor holding capacity. All holding capacities were measured in direct uplift using a calibrated hydraulic jack.

The results of the NWC, China Lake tests are given in Table 7.

Analysis of NWC Test Data

Eighteen tests were conducted in a weathered granite, and 12 tests were conducted in a vesicular basalt. The properties of these materials are given in Table 8.

Comparison of the tests, which were redundant with respect to the fluke and rock, indicates considerable variation in holding capacity even when similar conditions are maintained (compare tests 1, 2, and 6, tests 3 and 9, tests 4, 7, and 18). The most apparent reason for this variation is the amount of radial fracturing in the target caused by the penetration. These fractures relieve the normal stress on the projectile and result in lower holding capacities. The tendency to form radial cracks was greater in the dart-type projectiles than it was in the star, cone, and stake-type projectiles. Cracking was also greater when flukes were embedded in smaller outcrops or closer to the edge of large outcrops.

In basalt, all of the projectiles were damaged and would only penetrate if they impacted in an existing crack or joint. Two modified flukes were built. One design was a dart fluke with a blunter nose and a heavier after body, the other design was a heat-treated cone with the original nose shape and a heavier after body. The modified darts impacted, spalling off large pieces of rock, but did not penetrate. The heat-treated cones penetrated in both cases (tests 29 and 30) about one-half of their length. Even with a 4140 steel alloy fluke hardened to Rockwell C 34-36 to achieve excellent toughness characteristics, the nose was slightly bent.

The conical fluke was selected as the shape to use for all further rock tests. The frontal area of this shape increases evenly during penetration which continually compresses the surrounding rock. Because of this, the conical fluke had the greatest amount of surface area covered with a comminuted rock coating. This coated surface is the area of the projectile in which rock is actually bonded to the fluke due to the heat generated while penetrating. While this may or may not actually establish a rock-to-fluke bond, it certainly increases the surface roughness of the projectile and thus the frictional resistance to pullout.

The even increase in frontal area also eliminates the development of local high stress areas which lead to cracking of the rock, as was caused by the fins of the dart-type projectiles.

The final advantages of the conical projectile are more practical. It can be more easily forged in larger sizes and is amenable to heat treatment. The dart and star-type flukes have too much variation in cross-sectional thicknesses to permit heat treatment to the hardnesses required.

White Sands Missile Range Tests

Additional scale-model tests were conducted in 1978 using only the conical shaped projectile to establish a data base for developing a holding capacity equation. The tests were conducted by Sandia Laboratories at the White Sands Missile Range (WSMR) in outcrops of granite, basalt, limestone, sandstone, and shale. The same scale rock projectile was used as in the NWC tests; however, a larger piston was used because the Sandia launcher had a larger bore than the launcher used at NWC (see Figure 19).

Five rock flukes were shot into each of the five types of rock using Sandia Laboratories' pneumatic launcher (Figure 20). The flukes were then extracted using a calibrated hydraulic jack (Figure 21). Tests were made in direct uplift with displacement measured and plotted versus applied load. Core samples were taken at each test site and tested to determine properties. The properties of the rock at each site are given in Table 9.

Twenty-two of the 25 shots were embedded. Two of the three which did not penetrate were machined from bars which were cracked during heat treatment and so partially split upon impact. The third unsuccessful fluke was simply "rolled up" when it impacted the limestone target. Six of the 22 flukes which were embedded sustained damage to the base or were embedded at an angle which prevented pullout tests. These six were not extracted until 6 months later. To achieve extraction of these flukes, an attachment was welded to the fluke's base and then they were jacked out vertical to the rock surface. There is some doubt as to the

meaningfulness of this data because the embedded flukes were exposed to wetting and drying and freezing and thawing over the six-month period of their embedment. Finally they were heated to 315°C during welding. These actions should reduce the holding capacity of the flukes. This, in turn, would make estimates obtained from equations developed from the data base conservative.

There is one other possible mechanism, creep, which could reduce the holding capacity over a period of time. The effect of this factor was not explored in these tests.

The results of the WSMR tests are given in Table 10. Figures 22, 23, 24, 25, and 26 show typical fluke embedments and the post-extraction appearance of flukes for granite, basalt, limestone, sandstone, and shale, respectively. Note the relative degrees of damage to the target rocks caused by the embedment. Radial cracking was absent in all cases except the limestone. The granite tended to spall and crater on the weathered surface layer. The basalt damage was limited to the area impacted by the fluke and the larger diameter piston. The limestone, the most difficult target to penetrate, showed minimal amounts of surface damage. Successful embedments in the rock occurred where the rock surface was closely jointed or the fluke impacted near a joint. The sandstone was badly damaged by impact; the rock was shattered into 12-inch to 3-inch-sized blocks. The shale, which was very brittle and thin-bedded, was extensively cratered and shattered into 3-inch to 1/2-inch fragments. It was impossible to prepare a suitable compression test specimen from the shale core sample.

Analysis of White Sands Missile Range Data

If the tests in which the fluke failed to embed and the tests in which no effective holding capacity was developed are termed "unsuccessful," we can say that 100% of the granite tests, 80% of the basalt tests, 60% of the limestone tests, and 40% of the sandstone tests were successful. "Success" in this case being an embedded fluke which provided some measurable holding capacity. Table 11 lists these successful tests and their measured holding capacities. It also gives the mean holding (H) capacity and standard deviation (σ) for each rock type and for the collective data.

It can be observed from Table 11 that the holding capacity one may reasonably expect by shooting the rock fluke into an unknown type of rock is highly variable. The mean of all the listed tests is 54.97 kN. The standard deviation is 49.2 kN. One could say with 83% certainty that the anchor holding capacity would exceed 5.77 kN. The accuracy can be improved if one knows the test was conducted in granite, basalt, limestone, sandstone, or shale.

The holding capacities even in a single rock type show fairly wide variations. Properties of the rock types were obtained from a single core sample taken in the rock outcrop, with the test shots being made in the same outcrop usually within 15 feet of the core. The granite target was an exception. Tests 1-1, 1-2, and 1-3 were performed in the same granite outcrop but 70 to 80 feet away from the part that was cored. Although the material properties of the various rocks are probably the same within such short distances from the core, the properties of the

rock mass must change enough to account for the variation in the test results. For example, the material properties of the rock at two sites could be identical, but if one test is conducted near a joint and the other in a fairly intact portion of the outcrop, the test results would be quite different.

In an actual emplacement of the CEL-type embedment anchors, the anchors are fired upon touchdown. No provision is made for precise positioning of the anchor before firing. Thus, a similar variation in possible holding capacities should be expected.

Another source of the variation of holding capacities within one rock type is the deformation to the fluke. The amount of damage to the fluke in each test is described in Table 10. It was impossible to assess the influence such deformation has on the fluke's holding capacities, so it was ignored as an individual factor.

Development of Empirical Holding Capacity Equation for Rock Seafloors

Simple regressions of each target property versus holding capacity were performed as a first attempt at predicting anchor holding capacities. A computer program was used which evaluates the statistics of eight different forms of equations the simple regression may assume. The program then selects which equation best fits the data based upon the standard error of estimate and correlation coefficient.

The best evidence of existing relations was found between holding capacity (H) and Poisson's ratio (μ), H and Youngs modulus (E), and H and the rock quality designation (R') in decreasing order of correlation. The correlation with unconfined compressive strength (σ), unit weight (ρ), and porosity (p) were low. The simple regression procedure was also applied individually to the maximum embedded diameter of the fluke (D), the embedded length (L), and the embedded surface area (A_s). All of these had a low correlation to the holding capacity. Table 12 presents the results of the simple regressions.

Use of any of the equations listed in Table 12 for μ , E , or R' results in a lower standard error of estimate than the standard deviation for all tests given in Table 11. This means that knowing any one of these properties and applying the appropriate regression equation allows one to make a more confident prediction of the anchor's holding capacity. These equations will also allow some interpolation since the properties of targets other than the rocks tested may be substituted into the equation.

Further improvement in the accuracy of predictions may be possible by combining various independent variables in one function. The prediction method should also have some factor or physical fluke dimension included to allow extrapolation to larger size rock flukes. Trial equations were developed using the multiple linear regression method of Tolson (1970). The earlier trials are based upon results of polynomial regressions conducted on the relationship of individual independent variables to holding capacity. The various powers used are based upon those results. The combinations of variables used were based upon results from earlier trials.

Table 13 contains the results of the trials. Note that some of the equations were developed from a set of 14 data points (White Sands tests) and some from 16 data points (White Sands tests plus two data

points from the NWC, China Lake tests). The NWC data and the WSMR shale data could not be used in some trials because of a lack of data on some of the variables. Trials developed from 16 data points which appeared significant were also developed using 14 data points to afford comparison with other trials.

Independent variables used to develop the trial equations are:

D = maximum embedded diameter of the fluke, cm
L = maximum embedded length of the fluke, cm
 σ = unconfined compressive strength of target, MPa
 ρ = unit weight of target, g/cm³
E = Young's modulus of target, GPa
 μ = Poisson's ratio for target
R = Rock Quality Designation for target
p = porosity of target material, percent
z = depth of crater in target following embedment, cm
m = projectile mass, kg
v = projectile velocity, m/s

Trials number 1 through 11 explored equations that used only the independent variables which were properties of the target rock. Most of these trial equations reduce the range of the 83% confidence interval given in Table 11 for all the data. They have two failings, however: (1) they do not contain any variables which account for the variability between holding capacity in the individual targets, and (2) they do not contain any variables which allow the projectile size to be varied.

Trials 12 through 30 use various powers of the maximum embedded diameter, D, and the embedded length, L, with the variables describing target properties. Trials 31 through 34 use the projectile mass, m, and impact velocity, v, as the projectile descriptive variables. D and L are effective in correcting the two failings mentioned above; m and v, however, are the same in almost all of the tests and so do not improve the predictions of the earlier trials.

Development of trial equations 35-40 followed a different path than the previous trials. A trial equation was developed from a theoretical viewpoint. It was assumed that the holding capacity is a function of the residual stress in the rock acting on the embedded surface area of the fluke. Dividing the modulus, E, of the target rock by the Poisson's ratio, μ , for the rock will give the stress per unit lateral strain for elastic conditions. The amount of lateral strain induced would in turn be a function of the volume of rock displaced by the fluke.

Holding capacity, H = f (embedded surface area x residual stress)

If the fluke is idealized as a simple right circular cone,

$$H = k_1 \frac{\pi}{2} D \left(\frac{D^2}{4} + L^2 \right)^{1/2} \left[E \mu^{-1} \left(\frac{\pi}{12} D^2 L \right) \right]$$
$$H = k'_1 E \mu^{-1} D^3 L \left(\frac{D^2}{4} + L^2 \right)^{1/2}$$

where k_1, k'_1 = constants

E = Young's modulus, GPa

μ = Poisson's ratio

D = maximum embedded diameter, cm

L = embedded length, cm

This equation can be expressed in a form amenable to the multiple regression methods outlined earlier by taking the log of both sides

$$\log H = k + \log E - \log \mu + 3 \log D + \log L + \frac{1}{2} \log \left(\frac{D^2}{4} + L^2 \right)$$

The preceding considers only elastic conditions. The embedment in natural rock targets is not strictly elastic. Targets which are jointed, fractured, or in which porosity is significant are less likely to develop residual stresses. This effect was included in the above equation by multiplying by the rock quality designation R' (trial 36). This is the percent length of a core sample which is composed of sections longer than four inches. Thus rock with a large number of joints will have a low RQD value. The RQD does not take into effect porosity, p , of the rock which also tends to prevent the development of residual stresses. So $1-p$ was used to factor in this influence in trial 37.

One other parameter was tested in an attempt to combine the effects of porosity and fracturing. This is the depth of the crater, z , created by impact (trial 38). The volume of the crater would describe the rock condition better; however, the only measurements of the crater taken were depth.

Trials 41 and 42 were based upon the earlier findings of polynomial regressions performed on the relationship of embedded surface area to holding capacity. The best fit was a third order equation. Cubing the expression for volume and then adding the target properties which determine state of stress results in the combination of variables shown.

Equation 41 had the highest correlation of those tried. The standard error of estimate is quite high compared to others. The equation with the lowest standard error of estimate was number 8. The trend seemed to be that the simpler the equation, the lower the standard error of estimate. The more complex the equation, the higher the correlation coefficient. In fact, none of the trial equations had an error of estimate lower than that found in the simple regression between Poisson's ratio, μ , and holding capacity.

Because the best simple regression was found between Poisson's ratio and holding capacity, the regression was repeated after normalizing the holding capacities by the kinetic energy of the flukes. This changes the coefficients in the equation, but not the statistical evaluation.

The trial equation with the best fit to the test data with respect to minimizing the standard error of estimate would be then

$$H = \frac{1}{2} mv^2 * \mu * 1.96 \times 10^{-3} \quad (43)$$

This equation makes allowance for use with larger size projectiles through the kinetic energy term. The trial equation with the lowest standard error of estimate which does include a variable relating to projectile size is Equation 15:

$$H = 43.01 - 195.18 D + 21.42 L - 1.00 \sigma + 142.36 \rho \quad (15)$$

Equation 41 results in the highest correlation coefficient followed closely by Equations 26 and 28.

$$H = -27,799.65 + 1.40 D^6 - 935.67 D^2 - 0.40 L^3 + 602.48 L \\ - 18.25 E + 1,631.57 \mu + 12,929.01 \left(\frac{R}{100} \right) \\ + 24,547.86(1-p) \quad (41)$$

A 20K embedment anchor rock fluke has been designed and is shown in Figure 27. This fluke will be tested in Fiscal Year 80. Equations 15, 41, and 43 were applied to see what holding capacities would be predicted for this larger fluke. Full embedment of the 20K rock fluke to the protective collar was assumed. Equations 15 and 41 extrapolated very poorly to this anchor size. Equation 43 gave results that seem in the right order of magnitude (1.78 MN to 0.250 MN (400 to 56 kips) as the rock was varied from granite to sandstone (Table 14)).

Equations 26, 32, and 34 were also tried. Equation 26 gave predictions that seem too high and that did not vary with rock type. Equation 34 gave predictions that seem too low (94.1 to 4.02 kN). Results from Equation 32 seem of the right magnitude, but as with Equation 26, the predictions varied little as rock type changed. This lack of variation seems to be a weakness with Equation 32 because the WSMR tests results seemed to be quite strongly influenced by rock properties.

The risks of extrapolating any of the equations beyond the as yet narrow data base are apparent. At present it seems that Equation 43 or a similar equation offers the best hope for developing a general equation to predict holding capacity in rock. The form of Equation 43, where the fluke's kinetic energy has been normalized into the holding capacity, needs to be tried with other rock parameters, combinations of rock parameters, and with the inclusion of different anchor sizes.

SUMMARY

A review of available information on propellant-embedded anchor tests and installations in coral seafloors revealed that with few exceptions, insufficient data were gathered to allow analysis of results or to develop predictive procedures. Therefore, to develop holding capacity predictive procedures, a series of tests was conducted in coral at Barbers Point, Hawaii, using the CEL 10K propellant-embedded anchor; anchor, coral, embedment, and anchor pull parameters were measured. Also, a number of CEL 20K anchors that had been previously installed in coral at BARSTUR, Hawaii, were pull tested. In addition to these full-scale tests, two model-scale tests were conducted in a chalky limestone. Most of the pull tests ended in mechanical component failures rather than fluke extractions. A series of simple regression analyses of the various parameters measured indicated that the most important factors controlling holding capacity were fluke mass and velocity. Using only the tests where flukes were extracted, an equation for predicting holding capacity was developed as a function of kinetic energy.

Considerably fewer data are available on propellant-embedded anchors tested in rock seafloors than coral seafloors. Success has been mixed, with performance ranging from a failure of the fluke to embed to capacities exceeding the mechanical limits of the connective components and downhaul cables. Work on holding capacity in rock began with a series of model tests at NWC, China Lake, designed to study the ballistic and fluke characteristics that affect penetration. Seven different flukes were tested in a variety of rock types. A conical shaped fluke gave the most consistent performance in these tests. This fluke shape had less tendency to produce radial cracks in the rock which were observed to reduce holding capacity. Also, this shape has a uniformly increasing frontal area entering the rock surface which continually compresses the surrounding rock. As a result, this shape was observed to have larger surface areas covered with a comminuted rock coating than the other shapes. This coating is thought to contribute to frictional resistance to pullout.

Next, a series of model-scale tests were conducted at the White Sands Missile Range using the conical fluke shape in five rock types: basalt, limestone, granite, sandstone, and shale. Ballistic and fluke parameters were held constant. Penetration, rock fracturing, and holding capacity were observed to be dependent on rock type.

With the data from these tests as a base, trial predictive equations using selected anchor and rock parameters were tested against the data base. Some equations that resulted in a good fit to the data did not include fluke parameters that would allow for extrapolating the equation beyond the existing data base. A trial equation in which the holding capacities were normalized by the kinetic energy of the flukes offered both a best fit to the data and a means of extrapolating beyond the data base.

CONCLUSIONS

1. The best equation for predicting the holding capacity of propellant-embedded anchors in coral is:

$$H = 0.024 \left[\frac{1}{2} m v^2 \right]^{0.684}$$

where H = holding capacity, kN

m = projectile mass, kg

v = projectile velocity, m/sec

This equation is satisfactory for predicting the holding capacity of all the CEL propellant-embedded anchors. The single-sided lower 90% confidence limit is 45.3% of the predicted value. The use of this equation is limited to the range of parameters included in the data from which it was developed. It should not be applied to fluke shapes other than the CEL plate-like coral fluke. It should be applied with caution to installations in coral where properties are outside the limits of the data base. This equation could be improved by including the effect of coral strength.

2. An equation of the form

$$H = \frac{1}{2} m v^2 [f(\mu, \sigma, \rho, \dots)]$$

offers the best possibility of developing a general equation for predicting holding capacity in rock. An equation of this form will allow extrapolation to other anchor sizes. No trial equation gave suitable predictions for anchor sizes beyond the model scale used to acquire the data base. Data from full-scale 10K, 20K, 100K, and 300K propellant-embedded anchors will be necessary to develop a satisfactory equation.

3. Variations within each rock type tested had a large influence on performance. Of the 25 model tests performed in rock at White Sands Missile Range, only three flukes failed to embed, but three others provided minimal resistance to pullout. In each rock type where a poor result was observed, good results were also observed. In actual operational scenarios, provisions will be needed to accommodate an expected percentage of failures.

RECOMMENDATIONS

1. The equation for predicting holding capacity could be improved by including the effect of coral strength. It is recommended that such an improvement be made by:

- a. Collecting more data as a part of every future installation
- b. Using downhaul cables and mechanical connections strong enough to achieve pullout during testing
- c. Thoroughly documenting test parameters

2. It is recommended that data be gathered from full-scale anchor tests in rock to provide an expanded data base for developing an equation to predict holding capacity in rock. These tests should:

- a. Include as many anchor sizes as possible
- b. Include tests where a given anchor is operated at different kinetic energies
- c. Be done in several rock types
- d. Use downhauls and mechanical connections strong enough to achieve pullout
- e. Thoroughly document test parameters

REFERENCES

Beard, R. M., and J. F. Wadsworth (1976). Research and development program for anchoring in rock and coral seafloors. Civil Engineering Laboratory, Technical Memorandum M-42-76-8. Port Hueneme, Calif., May 1976.

Bradley, W. D. (1963). Field tests to determine the holding capacity of explosive embedment anchors. Naval Ordnance Laboratory, NOLTR 63-117. White Oak, Md., Jul 1963.

Ezekiel, M. (1949). Methods of correlation analysis, Second ed. New York, N.Y., John Wiley and Sons, 1949.

Mayo, H. C. (1973). Explosive embedment anchors for ship mooring. U. S. Army Mobility Equipment Research and Development Center, Report 2078. Fort Belvoir, Va., Nov 1973.

Smith, J. E. (1971). Explosive anchor for salvage operations - Progress and status. Naval Civil Engineering Laboratory, Technical Note N-1186. Port Hueneme, Calif., Oct 1971.

Taylor, R. J. (1976). CEL 20K propellant-actuated anchor. Civil Engineering Laboratory, Technical Report R-837. Port Hueneme, Calif., Mar 1976.

Tolson, W. E. (1970). A study of the vertical withdrawal resistance of projectile anchors. Thesis for Master of Science in Civil Engineering, Texas A&M University. College Station, Tex., May 1970.

True, D. G. (1977). Use of the CEL 100K propellant anchor to provide pulling reactions for toppling the Argus Island tower. Civil Engineering Laboratory, Technical Memorandum M-42-77-1. Port Hueneme, Calif., Apr 1977.

True, D. G., and R. J. Taylor (1976). The CEL 100K propellant actuated anchor - Utilization for tanker moorings in soft coral at Diego Garcia. Civil Engineering Laboratory, Technical Note N-1446. Port Hueneme, Calif., Jul 1976.

USS FRANK KNOX (DDR-742) Stranding Salvage. Naval Ship Systems Command, NAVSHIPS 0994-002-6010. Washington, D.C., 1968.

Valent, P. J. (1973). Design considerations for seafloor foundations on rock. Naval Civil Engineering Laboratory, Technical Note N-1281. Port Hueneme, Calif., Jun 1973.

Volk, W. (1958). Applied statistics for engineers. New York, N.Y., McGraw-Hill Book Co., 1958.

Wadsworth, J. F. (1976). Anchoring in rock - A preliminary study. Civil Engineering Laboratory, Technical Memorandum M-42-76-5. Port Hueneme, Calif., Apr 1976.

Wadsworth, J. F., and R. J. Taylor (1976). CEL 10K propellant-actuated anchor. Civil Engineering Laboratory, Technical Note N-1441. Port Hueneme, Calif., Jun 1976.

Young, C. W. (1967). The development of empirical equations for predicting depth of an earth-penetrating projectile. Sandia Laboratories, Report no. SC-DR-67-60. Albuquerque, N.M., May 1967.

Table 1. Data on Coral Embedment Anchors Prior to 1978

Test No.	Location	Type Embedment Anchor	Fluke Type	Penetration (m)	Angle of Loading (deg)	Holding Capacity, H (kN)	Unconfined Compressive Strength (MPa)	Mode of Failure	Remarks
1	Key West, FL	SEASTAPLE	MKV	0.76	0	3.12	unknown	downhaul failed	Mar 1961 (Bradley, 1963)
2		SEASTAPLE	MKV	0.76	0	2.23	unknown	pulled out	Mar 1961 (Bradley, 1963)
3		MERDC XM-50	Sediment	5.8	0.45	289.3	unknown	pulled out	May 1963 (Mayo, 1973)
4		MERDC XM-50	Sediment	7.3	0.45	356	unknown	pulled out	May 1963 (Mayo, 1973)
1		MERDC XM-200	Sediment	5.3	11	645.3	unknown	keying flap failure	Mar 1963 (Mayo, 1973)
2		MERDC XM-200	Sediment	5.6	11	267	unknown	keying flap failure	May 1963 (Mayo, 1973)
3		MERDC XM-200	Sediment	6.0	11	445	unknown	keying flap failure	May 1963 (Mayo, 1973)
4		MERDC XM-200	Sediment	6.5	45	956.8	unknown	keying flap failure	May 1963 (Mayo, 1973)
7		MERDC XM-200	Sediment	3.3	0	979	unknown	keying flap failure	May 1963 (Mayo, 1973)
12	Barbers Point, HI	SUPSAVL	Coral 1	2.4	>80	302.6	10.35 to 17.25	pulled out	May 1968 (Smith, 1971)
13		SUPSAVL	Coral 2	2.1	>80	534	1.35 to 17.25	pulled out	Jul 1968 (Smith, 1971)
14		SUPSAVL	Coral 2	3.4	>80	605	1.35 to 17.25	pulled out	Jul 1968 (Smith, 1971)
22	Bermuda	SUPSAVL	Coral 2	2.7	80	289.3	10.35 to 17.25	pulled out	Apr 1969 (Smith, 1971)
23		SUPSAVL	Coral 2	3.4	80	334+	10.95 to 1.25	unable to extract	Apr 1969 (Smith, 1971)
24		SUPSAVL	Coral 2	3.5	80	334+	10.35 to 1.25	unable to extract	Apr 1969 (Smith, 1971)
25		SUPSAVL	Coral 2	3.5	80	668+	10.35 to 1.25	unable to extract	Apr 1969 (Smith, 1971)
17		MAGNAVOX	Stub Nose	0.38	0	0.9	unknown	pulled out	Jun 1964
21		MAGNAVOX	Long Nose	0.50	0	3.4	unknown	pulled out	Jun 1964
23		MAGNAVOX	Long Nose	0.38	60	7.1	unknown	downhaul failed	Jul 1964
28		MAGNAVOX	Long Nose	0.61	30	4.0	unknown	downhaul failed	Aug 1964
1	Midway Island	CEL 10K	Sand	2.7	~70	(est.) 130+	unknown	placed as mooring	
2		CEL 10K	Mud	4.3	~70	(est.) 130+	unknown	for USS DIVER (ARS)	
3		CEL 20K	Sand	0.9	~70	(est.) 130+	unknown	Sep 1975	
4		CEL 20K	Sand	4.3	~70	(est.) 130+	unknown	(Wadsworth and Taylor, 1976)	
5		CEL 20K	Sand	3.1	~70	(est.) 130+	unknown		

continued

Table 1. Continued

Test No.	Location	Type Embedment Anchor	Fluke Type	Penetration (m)	Angle of loading (deg)	Holding Capacity, H (kN)	Unconfined Compressive Strength (MPa)	Mode of failure	Remarks
P-1	Diego Garcia Island	CEL 100K	Coral 3	10.7	0	490+	2.7-3.6 (est.)	placed as permanent POL mooring for tankers May 1975 (True and Taylor, 1976)	
		CEL 100K	Coral 3	7.9	0	490+	2.7-3.6 (est.)		
		CEL 100K	Coral 3	10.7	0	490+	2.7-3.6 (est.)		
		CEL 100K	Coral 3	10.7	0	490+	2.7-3.6 (est.)		
		CEL 100K	Coral 3	9.5	0	490+	2.7-3.6 (est.)		
		CEL 100K	Coral 3	10.7	0	490+	2.7-3.6 (est.)		
		CEL 100K	Coral 3	9.2	0	668+	2.7-3.6 (est.)		
		CEL 100K	Coral 3	9.2	0	490+	2.7-3.6 (est.)		
		CEL 100K	Coral 3	10.7	0	490+	2.7-3.6 (est.)		
		CEL 100K	Coral 3	9.5	0	490+	2.7-3.6 (est.)		
P-10	Diego Garcia Island	CEL 100K	Coral 3	10.7	0	490+	2.7-3.6 (est.)	placed as temporary POL mooring for tankers Jun 1975 (True and Taylor, 1976)	
		CEL 100K	Sand/Clay	8.5	0	734+	2.7-3.6 (est.)		
		CEL 100K	Coral 3	8.5	0	490+	2.7-3.6 (est.)		
		CEL 100K	Sand/Clay	8.5	0	490+	2.7-3.6 (est.)		
		CEL 100K	Sand/Clay	9.8	0	490+	2.7-3.6 (est.)		
		CEL 100K	Sand/Clay	9.2	0	490+	2.7-3.6 (est.)		
		CEL 100K	Sand/Clay	8.9	0	490+	2.7-3.6 (est.)		
		CEL 100K	Sand/Clay	9.2	0	490+	2.7-3.6 (est.)		
		CEL 100K	Piston	9.2	0	311.5	2.7-3.6 (est.)		
		CEL 100K	Piston	9.2	0	213.6	2.7-3.6 (est.)		
T-1	Diego Garcia Island	CEL 100K	Piston	9.2	0	222.5	2.7-3.6 (est.)	pistons recovered for reuse after indicated installations (True and Taylor, 1976)	
		CEL 100K	Piston	7.9	0	400.5	2.7-3.6 (est.)		
		CEL 100K	Piston	9.2	0	222.5	2.7-3.6 (est.)		
		CEL 100K	Piston	7.6	0	445	2.7-3.6 (est.)		
		CEL 100K	Piston	7.6	0	356	2.7-3.6 (est.)		
		CEL 100K	Piston	9.2	0	222.5	2.7-3.6 (est.)		
		CEL 100K	Piston	7.9	0	356	2.7-3.6 (est.)		
		CEL 100K	Piston	9.2	0	155.8	2.7-3.6 (est.)		
		CEL 100K	Piston	6.4	0	155.8	2.7-3.6 (est.)		
		CEL 100K	Piston	7.0	0	155.8	2.7-3.6 (est.)		

continued

Table 1. Continued

Test No.	Location	Type Embedment Anchor	Fluke Type	Penetration (m)	Angle of Loading (deg)	Holding Capacity, H (kN)	Unconfined Compressive Strength (MPa)	Mode of Failure	Remarks
1	Argus Island	CEL 100K	Coral 1	est. 2.3	72	—	35.70 (est.)	left embedded connecting shackle	placed as ARS mooring
2		CEL 100K	Coral 1	est. 2.3	72	—	35.70 (est.)	left embedded	placed as ARS mooring
3		CEL 100K	Coral 4	est. 2.3	72	—	35.70 (est.)	left embedded	placed as ARS mooring
4		CEL 100K	Coral 4	est. 2.3	84	556+	35.70 (est.)	pulling to topple	measured loads while
5		CEL 100K	Coral 4	est. 2.3	84	556+	35.70 (est.)	Argus Island tower	placed as ARS mooring
6		CEL 100K	Coral 3	est. 2.3	84	556+	35.70 (est.)	Apr 1976	measured loads while
7		CEL 100K	Coral 4	est. 2.3	84	556+	35.70 (est.)	(True, 1977)	pulling to topple
M-1A	Barking Sands, HI	CEL 20K	Coral	1.2	80	(est.) 75+	unknown	proof load	placed as mooring for
M-1B		CEL 20K	Coral	1.5	80	(est.) 75+	unknown	proof load	cable laying ship
M-2A		CEL 20K	Coral	—	80	(est.) 75+	unknown	proof load	long lines
M-2B		CEL 20K	Coral	—	80	151+	unknown	proof load	Aug 1976
M-3A		CEL 20K	Coral	2.7	80	(est.) 75+	unknown	proof load	
M-3B		CEL 20K	Coral	1.2	80	(est.) 75+	unknown	proof load	
M-4A		CEL 20K	Coral	0.9	80	107+	unknown	proof load	
M-4B		CEL 20K	Coral	2.7	80	(est.) 75+	unknown	proof load	
M-5A		CEL 20K	Coral	2.4	80	(est.) 75+	unknown	proof load	
M-5B		CEL 20K	Coral	3.7	80	(est.) 75+	unknown	proof load	

Table 2. CEL 10K Coral Anchor Test Data From Barbers Point, Oahu

[Anchors were installed and pulled in June 1978.]

Test No.	Type Embedment Anchor	Fluke Type	Penetration (m)	Angle of Loading From Vertical (deg)	Holding Capacity, H (kN)	Unconfined Compressive Strength (MPa)	Average Bulk Density (g/cm ³)	Mode of Failure	Remarks
1	CEL 10K	Coral	0.48	68	156+	29	1.98	Downhaul failed	
2	CEL 10K	Coral	0.61	68	180+	29	1.98	Downhaul failed	
3	CEL 10K	Coral	0.61	68	140+	29	1.98	Downhaul failed	
4	CEL 10K	Coral	0.46	68	174+	29	1.98	Downhaul failed	
5	CEL 10K	Coral	0.53	68	4.5 ^a	29	1.98	Downhaul failed	
6	CEL 10K	Coral	0.38	68	162.0	29	1.98	Pull out	
7	CEL 10K	Coral	0.48	0	100+	29	1.98	Downhaul failed	
8	CEL 10K	Coral	0.92	0	105.0	29	1.98	Pull out	
9	CEL 10K	Coral	1.68	82	223+	29	1.98	Downhaul failed	
10	CEL 10K	Coral	1.83	82	220+	29	1.98	Downhaul failed	
11	CEL 10K	Coral	2.14	82	No data	29	1.98	Pull out	
12	CEL 10K	Coral	1.98	82	131+	29	1.98	Shackle failed	Load cell not connected

^aProof load was higher (estimated as 20 kN) than measured test load.

Table 3. CEL 20K Coral Anchor Test Data From BARSTUR, Kauai

Test No.	Type Embedment Anchor	Fluke Type	Penetration (m)	Angle of Loading From Vertical (deg)	Holding Capacity, H (kN)	Average Unconfined Compressive Strength (MPa)	Average Bulk Density (g/cm ³)	Mode of Failure	Remarks
M-3A	CEL 20K	Coral	2.7	45	231+	23.8	2.59	Downhaul failed	Anchors installed
-3B	CEL 20K	Coral	1.2	45	178+	23.8	2.59	Downhaul failed	Aug 1976; used as
M-4A	CEL 20K	Coral	0.9	0	178+	23.8	2.59	Downhaul failed	mooring Sep 1976;
-4B	CEL 20K	Coral	2.7	0	249+	23.8	2.59	Downhaul failed	downhauls laid on
M-5A	CEL 20K	Coral	2.4	0	142+	23.8	2.59	Downhaul failed	bottom until pull
-5B	CEL 20K	Coral	3.7	20	205+	23.8	2.59	Downhaul failed	tested in Sep 1978

^a + indicates highest load anchor experienced before some other component failed.

Table 4. Data Available on Performance of Embedment Anchors in Coral

Test No.	Type of Anchor	Test Location	Fluke Type	Projectile Mass, M (kg)	Muzzle Velocity, V (m/s)	Frontal Area, F (cm ²)	Angle of Loading, θ (deg)	Embedded Surface Area, A (m ²)	Target, σ_u (MPa)	Target Density, ρ (g/cm ³)
1	SEASTAPLE	Key West	MK V	unknown	unknown	unknown	0	0.1277	unknown	unknown
2 ^a	SEASTAPLE	Key West	MK V	unknown	unknown	unknown	0	0.1277	unknown	unknown
3 ^a	MERDC	Key West	Sediment	102	107	73	0	1.3468	unknown	unknown
4 ^a	XM-50	Key West	Sediment	102	107	73	0	1.3468	unknown	unknown
1	MERDC	Key West	Sediment	408	138	271	11	4.3215	unknown	unknown
2	XM-200	Key West	Sediment	408	125	271	11	4.3215	unknown	unknown
3	XM-200	Key West	Sediment	408	138	271	11	4.3215	unknown	unknown
4	XM-200	Key West	Sediment	408	97	271	45	4.3215	unknown	unknown
7	XM-200	Key West	Sediment	408	97	271	0	4.3215	unknown	unknown
12 ^a	SUPSLV	Key West	Coral 1	815	46	892	>80	4.3299	not measured	unknown
13 ^a	SUPSLV	Key West	Coral 2	815	46	892	>80	4.3299	not measured	unknown
14 ^a	SUPSLV	Key West	Coral 2	815	46	892	>80	4.3299	not measured	unknown
22 ^a	SUPSLV	Barbers Point	Coral 2	815	73	892	>80	4.3299	10.4-17.3	unknown
23	SUPSLV	Barbers Point	Coral 2	815	85	892	>80	4.3299	10.4-17.3	unknown
24	SUPSLV	Barbers Point	Coral 2	815	85	892	>80	4.3299	10.4-17.3	unknown
25	SUPSLV	Barbers Point	Coral 2	815	85	892	>80	4.3299	10.4-17.3	unknown
1 ^a	CEL 10K	Midway Island	Sand	67	120	~100	~70	0.4167	unknown	unknown
2	CEL 10K	Midway Island	Mud	78	116	~100	~70	0.7327	unknown	unknown
3	CEL 20K	Midway Island	Sand	136	120	~150	~70	0.9985	unknown	unknown
4 ^a	CEL 20K	Midway Island	Sand	136	120	~150	~70	0.9985	unknown	unknown
5	CEL 20K	Midway Island	Sand	136	120	~150	~70	0.9985	unknown	unknown
P-1	CEL 100K	Diego Garcia	Coral 3	725	133	unknown	0	3.4146	unknown	unknown
P-2	CEL 100K	Diego Garcia	Coral 3	725	131	unknown	0	3.4146	unknown	unknown
P-3	CEL 100K	Diego Garcia	Coral 3	725	127	unknown	0	3.4146	unknown	unknown
P-4	CEL 100K	Diego Garcia	Coral 3	725	127	unknown	0	3.4146	unknown	unknown
P-5	CEL 100K	Diego Garcia	Coral 3	725	120	unknown	0	3.4146	unknown	unknown
P-6	CEL 100K	Diego Garcia	Coral 3	725	120	unknown	0	3.4146	unknown	unknown
P-7	CEL 100K	Diego Garcia	Coral 3	725	—	unknown	0	3.4146	unknown	unknown
P-8	CEL 100K	Diego Garcia	Coral 3	725	130	unknown	0	3.4146	unknown	unknown
P-9	CEL 100K	Diego Garcia	Coral 3	725	128	unknown	0	3.4146	unknown	unknown
P-10	CEL 100K	Diego Garcia	Coral 3	725	—	unknown	0	3.4146	unknown	unknown
T-1	CEL 100K	Diego Garcia	Coral 3	725	125	unknown	0	3.4146	unknown	unknown
T-2	CEL 100K	Diego Garcia	Sand/Clay	884	102	unknown	0	5.2077	unknown	unknown
T-3	CEL 100K	Diego Garcia	Coral 3	725	125	unknown	0	3.4146	unknown	unknown
T-4	CEL 100K	Diego Garcia	Sand/Clay	884	108	unknown	0	5.2077	unknown	unknown
T-5	CEL 100K	Diego Garcia	Sand/Clay	884	110	unknown	0	5.2077	unknown	unknown
T-6	CEL 100K	Diego Garcia	Sand/Clay	884	110	unknown	0	5.2077	unknown	unknown
T-7	CEL 100K	Diego Garcia	Sand/Clay	884	107	unknown	0	5.2077	unknown	unknown
T-8	CEL 100K	Diego Garcia	Sand/Clay	884	102	unknown	0	5.2077	unknown	unknown

Data Available on Performance of Embedment Anchors in Coral

Zuzzle Velocity, V (m/s)	Frontal Area, F (cm ²)	Angle of Loading, θ (deg)	Embedded Surface Area, A (m ²)	Target, σ_u (MPa)	Target Density, ρ (g/cm ³)	Holding Capacity, H (kN)	Remarks
unknown	unknown	0	0.1277	unknown	unknown	3.12+	Mar 1961; downhaul failed
unknown	unknown	0	0.1277	unknown	unknown	2.23	Mar 1961; pulled out
107	73	0	1.3468	unknown	unknown	289.3	May 1963; pulled out
107	73	0	1.3468	unknown	unknown	356	May 1963; pulled out
138	271	11	4.3215	unknown	unknown	645.3+	Mar 1963; keying flap failed; pulled out
125	271	11	4.3215	unknown	unknown	267+	May 1963; keying flap failed; pulled out
138	271	11	4.3215	unknown	unknown	445+	May 1963; keying flap failed; pulled out
97	271	45	4.3215	unknown	unknown	956.8+	May 1963; keying flap failed; pulled out
97	271	0	4.3215	unknown	unknown	979+	May 1963; keying flap failed; pulled out
46	892	>80	4.3299	not measured	unknown	302.6	May 1968; pulled out
46	892	>80	4.3299	not measured	unknown	534	Jul 1968; pulled out
46	892	>80	4.3299	not measured	unknown	605	Jul 1968; pulled out
73	892	>80	4.3299	10.4-17.3	unknown	289.3	Apr 1969; pulled out
85	892	>80	4.3299	10.4-17.3	unknown	334+	Apr 1969; unable to extract
85	892	>80	4.3299	10.4-17.3	unknown	334+	Apr 1969; unable to extract
85	892	>80	4.3299	10.4-17.3	unknown	668+	Apr 1969; unable to extract
120	~100	~70	0.4167	unknown	unknown	not measured	Sep 1975; pulled out
116	~100	~70	0.7327	unknown	unknown	not measured	Sep 1975; left embedded
120	~150	~70	0.9985	unknown	unknown	not measured	Sep 1975; left embedded
120	~150	~70	0.9985	unknown	unknown	not measured	Sep 1975; pulled out
120	~150	~70	0.9985	unknown	unknown	not measured	Sep 1975; left embedded
133	unknown	0	3.4146	unknown	unknown	490+	May 1975; proof test; left embedded
131	unknown	0	3.4146	unknown	unknown	490+	May 1975; proof test; left embedded
127	unknown	0	3.4146	unknown	unknown	490+	May 1975; proof test; left embedded
127	unknown	0	3.4146	unknown	unknown	490+	May 1975; proof test; left embedded
120	unknown	0	3.4146	unknown	unknown	490+	May 1975; proof test; left embedded
120	unknown	0	3.4146	unknown	unknown	490+	May 1975; proof test; left embedded
—	unknown	0	3.4146	unknown	unknown	668+	May 1975; proof test; left embedded
130	unknown	0	3.4146	unknown	unknown	490+	May 1975; proof test; left embedded
128	unknown	0	3.4146	unknown	unknown	490+	May 1975; proof test; left embedded
—	unknown	0	3.4146	unknown	unknown	490+	May 1975; proof test; left embedded
125	unknown	0	3.4146	unknown	unknown	490+	May 1975; proof test; left embedded
102	unknown	0	5.2077	unknown	unknown	734+	May 1975; proof test; left embedded
125	unknown	0	3.4146	unknown	unknown	490+	May 1975; proof test; left embedded
108	unknown	0	5.2077	unknown	unknown	490+	May 1975; proof test; left embedded
110	unknown	0	5.2077	unknown	unknown	490+	May 1975; proof test; left embedded
110	unknown	0	5.2077	unknown	unknown	490+	May 1975; proof test; left embedded
107	unknown	0	5.2077	unknown	unknown	490+	May 1975; proof test; left embedded
102	unknown	0	5.2077	unknown	unknown	490+	May 1975; proof test; left embedded

continued

Table 4. Continued

Test No.	Type of Anchor	Test Location	Fluke Type	Projectile Mass, M (kg)	Muzzle Velocity, V (m/s)	Frontal Area, F (cm ²)	Angle of Loading, θ (deg)	Embedded Surface Area, A (m ²)	Target, σ_u (MPa)	Target Density, ρ (g/cm ³)
1	CEL 100K	Argus Island	Coral 1 MOD	—	—	unknown	72	5.2077	35-70 ^b	unknown
2	CEL 100K	Argus Island	Coral 1 MOD	—	—	unknown	72	5.2077	35-70	unknown
3	CEL 100K	Argus Island	Coral 4	680	—	unknown	72	2.9193	35-70	unknown
4	CEL 100K	Argus Island	Coral 4	657	134	unknown	84	2.9193	35-70	unknown
5	CEL 100K	Argus Island	Coral 4	657	134	unknown	84	2.9193	35-70	unknown
6	CEL 100K	Argus Island	Coral 3	661	133	unknown	84	3.4146	35-70	unknown
7	CEL 100K	Argus Island	Coral 4	680	130	unknown	84	2.9193	35-70	unknown
M-1A	CEL 20K	BARSTUR	Coral	127	122	153	80	1.1288	23.8	2.59
M-1B	CEL 20K	BARSTUR	Coral	127	122	153	80	1.1288	23.8	2.59
M-2A	CEL 20K	BARSTUR	Coral	127	122	153	80	1.1288	23.8	2.59
M-2B	CEL 20K	BARSTUR	Coral	127	122	153	80	1.1288	23.8	2.59
M-3A	CEL 20K	BARSTUR	Coral	127	122	153	45	1.1288	23.8	2.59
M-3B	CEL 20K	BARSTUR	Coral	127	122	153	45	1.1288	23.8	2.59
M-4A	CEL 20K	BARSTUR	Coral	127	122	153	0	1.1288	23.8	2.59
M-4B	CEL 20K	BARSTUR	Coral	127	122	153	0	1.1288	23.8	2.59
M-5A	CEL 20K	BARSTUR	Coral	127	122	153	0	1.1288	23.8	2.59
M-5B	CEL 20K	BARSTUR	Coral	127	122	153	20	1.1288	23.8	2.59
1	CEL 10K	Barbers Point	Coral	52	172	85	68	0.6437	29.1	1.98
2	CEL 10K	Barbers Point	Coral	52	172	85	68	0.7695	29.1	1.98
3	CEL 10K	Barbers Point	Coral	52	172	85	68	0.7695	29.1	1.98
4	CEL 10K	Barbers Point	Coral	52	172	85	68	0.6179	29.1	1.98
5 ^a	CEL 10K	Barbers Point	Coral	52	172	85	68	0.6934	29.1	1.98
6 ^a	CEL 10K	Barbers Point	Coral	52	172	85	68	0.5308	29.1	1.98
7	CEL 10K	Barbers Point	Coral	52	172	85	0	0.6437	29.1	1.98
8 ^a	CEL 10K	Barbers Point	Coral	52	172	85	0	0.7695	29.1	1.98
9	CEL 10K	Barbers Point	Coral	52	172	85	82	0.7695	29.1	1.98
10	CEL 10K	Barbers Point	Coral	52	172	85	82	0.7695	29.1	1.98
11	CEL 10K	Barbers Point	Coral	52	172	85	82	0.7695	29.1	1.98
12	CEL 10K	Barbers Point	Coral	52	172	85	82	0.7695	29.1	1.98
NWC-28 ^a	Scale Model	NWC, China Lake	Coral	2.3	140	12	0	0.0441	2.2	1.50
NWC-29 ^a	CEL 20K	NWC, China Lake	Coral	2.3	140	12	0	0.0631	2.2	1.50

^aData used to develop the empirical holding capacity equation.^bAverage: 52.5 MPa.

Table 4. Continued

Muzzle Velocity, V (m/s)	Frontal Area, F (cm ²)	Angle of Loading, θ (deg)	Embedded Surface Area, A (m ²)	Target, σ_u (MPa)	Target Density, ρ (g/cm ³)	Holding Capacity, H (kN)	Remarks
—	unknown	72	5.2077	35-70 ^b	unknown	not tested	Apr 1976; not tested; left embedded
—	unknown	72	5.2077	35-70	unknown	not tested	Apr 1976; not tested; left embedded
—	unknown	72	2.9193	35-70	unknown	not tested	Apr 1976; not tested; left embedded
134	unknown	84	2.9193	35-70	unknown	556+	Apr 1976; measured loads; left embedded
134	unknown	84	2.9193	35-70	unknown	556+	Apr 1976; measured loads; left embedded
133	unknown	84	3.4146	35-70	unknown	556+	Apr 1976; measured loads; left embedded
130	unknown	84	2.9193	35-70	unknown	556+	Apr 1976; measured loads; left embedded
122	153	80	1.1288	23.8	2.59	75+	Aug 1976; proof load; left embedded
122	153	80	1.1288	23.8	2.59	75+	Aug 1976; proof load; left embedded
122	153	80	1.1288	23.8	2.59	75+	Aug 1976; proof load; left embedded
122	153	80	1.1288	23.8	2.59	151+	Aug 1976; proof load; left embedded
122	153	45	1.1288	23.8	2.59	231+	Aug 1976; tested Aug 1978; downhaul broke
122	153	45	1.1288	23.8	2.59	178+	Aug 1976; tested Aug 1978; downhaul broke
122	153	0	1.1288	23.8	2.59	178+	Aug 1976; tested Aug 1978; downhaul broke
122	153	0	1.1288	23.8	2.59	249+	Aug 1976; tested Aug 1978; downhaul broke
122	153	0	1.1288	23.8	2.59	142+	Aug 1976; tested Aug 1978; downhaul broke
122	153	20	1.1288	23.8	2.59	205+	Aug 1976; tested Aug 1978; downhaul broke
172	85	68	0.6437	29.1	1.98	156+	Jun 1978; downhaul broke
172	85	68	0.7695	29.1	1.98	181+	Jun 1978; downhaul broke
172	85	68	0.7695	29.1	1.98	140+	Jun 1978; downhaul broke
172	85	68	0.6179	29.1	1.98	174+	Jun 1978; downhaul broke
172	85	68	0.6934	29.1	1.98	4.5	Jun 1978; anchor pulled out
172	85	68	0.5308	29.1	1.98	162	Jun 1978; anchor pulled out
172	85	0	0.6437	29.1	1.98	100+	Jun 1978; downhaul broke
172	85	0	0.7695	29.1	1.98	105	Jun 1978; anchor pulled out
172	85	82	0.7695	29.1	1.98	223+	Jun 1978; downhaul broke
172	85	82	0.7695	29.1	1.98	220+	Jun 1978; downhaul broke
172	85	82	0.7695	29.1	1.98	—	Jun 1978; downhaul broke; load not measured
172	85	82	0.7695	29.1	1.98	131+	Jun 1978; downhaul broke; load not measured
140	12	0	0.0441	2.2	1.50	21	Apr 1977; pulled out
140	12	0	0.0631	2.2	1.50	16	Apr 1977; pulled out

Table 5. Data on Coral Anchor Tests Where the Flukes Were Pulled Out

Test No.	Anchor	Location	Fluke Mass, m (kg)	Fluke Velocity, v (m/sec)	Fluke Frontal Area, F (cm^2)	Load Point Eccentricity	Angle of Loading, θ (deg)	Target Strength, σ (MPa)	Target Density, ρ (gm/cm^3)	Embedded Surface Area, A (cm^2)	Pullout Load, H (kN)	Fluke Type
1	Sea Staple	Key West	unknown	unknown	0	0	0	unknown	0.128	2.23	Mk V	
2	MERIC XM-50	Key West	102	107	73	0	0	unknown	1.347	289	sediment	
3	MERIC XM-50	Key West	102	107	73	0	0	unknown	1.347	356	sediment	
1	MERIC XM-200	Key West	408	138	271	0	11	unknown	4.32	645	sediment	
2	MERIC XM-200	Key West	408	125	271	0	11	unknown	4.32	267	sediment	
3	MERIC XM-200	Key West	408	138	271	0	11	unknown	4.32	445	sediment	
4	MERIC XM-200	Key West	408	97	271	0	45	unknown	4.32	957	sediment	
7	MERIC XM-200	Key West	408	97	271	0	0	unknown	4.32	979	sediment	
12	SUPSAVL	Key West	815	46	892	0	>80	unknown	4.33	303	coral 1	
13	SUPSAVL	Key West	815	46	892	0	>80	unknown	4.33	534	coral 2	
14	SUPSAVL	Key West	815	46	892	0	>80	unknown	4.33	605	coral 2	
22	SUPSAVL	Barbers Point	815	73	892	0	>80	13.8	unknown	4.33	289	coral 2
1	CEL 10K	Midway	67	120	100	0.25	~70	unknown	0.417	unknown	sand	
4	CEL 20K	Midway	136	120	150	0.25	~70	unknown	1.00	unknown	sand	
5	CEL 10K	Barbers Point	52	172	85	0.25	68	29.1	0.693	4.5	coral	
6	CEL 10K	Barbers Point	52	172	85	0.25	68	29.1	1.98	0.531	coral	
8	CEL 10K	Barbers Point	52	172	85	0.25	0	29.1	1.98	0.770	coral	
28	Model 20 K	China Lake	2.3	140	12	0.25	0	2.2	1.5	0.044	21	
29	Model 20 K	China Lake	2.3	140	12	0.25	0	2.2	1.5	0.063	16	

Table 6. Predicted Mean Holding Capacity and Holding Capacity Expected to Be Exceeded 90% of the Time for Each Anchor

Item	Anchor			
	CEL 10K	CEL 20K	CEL 100K	CEL 300K
Mean Holding Capacity (kN)	260	360	1,050	2,200
Holding Capacity Exceeded 90% of the Time (kN)	115	160	470	1,000

Table 7. Results of Scale Anchor Tests at NWC, China Lake

Test No.	Fluke Type	Projectile Mass (kg)	Impact Velocity (m/s)	KE (kJ)	Rock Type	Embedded Length (cm)	Holding Capacity (kN)	Crater Size Depth x Width (cm)	Radial Cracking
1	Dart	2.21	136	20.4	granite	16.5	56.5	5.1 x 12.7	none
2	Dart	2.21	120	15.9	granite	15.2	29.4	5.1 x 20.3	moderate
3	Serrate Dart	2.13	136	19.7	granite	12.7	13.1	5.1 x 12.7	extensive
4	Star	2.02	no data	-	granite	17.8	30.3	no crater	moderate
5	Cone	2.22	134	19.9	granite	10.1	89.0+	6.4 x 15.2	minor
6	Dart	2.21	139	21.3	granite	15.2	15.1	5.1 x 12.7	extensive
7	Star	2.02	124	15.5	granite	19	89.0+	3.8 x 12.7	none
8	Stake	1.93	140	18.9	granite	0	0	spall	-
9	Serrate Dart	2.13	123	16.1	granite	15.2	89.0+	5.0 x 13.0	none
10	Dart	1.88	152	21.7	granite	10.1	30.7	no crater	minor
11	Coral	2.31	141	23.0	granite	0	0	spall	-
12	Dart	1.88	no data	-	granite	14.0	29.4	no crater	minor
13	Dart	3.03	104	16.4	granite	20.4	47.2	no crater	none
14	Magnavox	-	120	-	granite	17.8	14.7	6.4 x 20.3	none
15	Stake	2.14	161	27.7	granite	7.6	20.6	8.9 x 20.3	none
16	Tapered Stake	2.09	171	30.6	granite	10.2	16.0	5.1 x 12.7	none

continued

Table 7. Continued

Test No.	Fluke Type	Projectile Mass (kg)	Impact Velocity (m/s)	KE (kJ)	Rock Type	Embedded Length (cm)	Holding Capacity (kN)	Crater Size Depth x Width (cm)	Radial Cracking
17	Serrate Stake	2.10	171	30.7	granite	10.2	23.5	5.1 x 12.7	none
18	Star	2.18	136	20.2	granite	15.2	58.7+	5.1 x 12.7	none
19	Serrate Dart	2.30	no data	-	basalt	0	0	5.1 x 7.6	none
20	Dart	2.37	123	17.9	basalt	14.0	3.5	no crater	embedded in existing crack
21	Dart	2.37	133	21.0	basalt	12.7	10.6	no crater	extensive
22	Dart	3.19	123	24.1	basalt	0	0	gouged	-
23	Dart	2.04	138	19.4	basalt	0	0	gouged	-
24	Star	2.18	144	22.6	basalt	17.8	22.9	no crater	embedded in existing crack
25	Serrate Stake	2.10	146	22.4	basalt	15.2	32.3	no crater	embedded in existing crack
26	Tapered Stake	2.09	no data	-	basalt	15.2	3.5	no crater	embedded in existing crack
27	Mod. Dart	2.82	no data	-	basalt	0	0	gouged	-

Table 7. Continued

Test No.	Fluke Type	Projectile Mass (kg)	Impact Velocity (m/s)	KE (kJ)	Rock Type	Embedded Length (cm)	Holding Capacity (kN)	Crater Size Depth x Width (cm)	Radial Cracking
28	Mod. Dart	2.82	no data	-	basalt	0	0	gouged	-
29	HT ^a Cone	2.81	no data	-	basalt	15.5	23.14	no crater	moderate
30	HT ^a Cone	2.81	no data	-	basalt	18.8	0	split rock	extensive

^aHT signifies heat treated.

Table 8. Properties of Rocks at NWC, China Lake Test Site

Sample No.	Rock Type	Density (g/cm ³)	Unconfined Compressive Strength (MPa)	Strain to Failure (%)	50% Tangent Modulus (GPa)
1	Basalt	2.324	48.8	1.12	5.0
2	Basalt	2.305	47.8	1.07	5.1
3	Basalt	2.271	29.7	0.84	4.1
4	Basalt	2.140	23.1	0.59	5.5
5	Granite	2.750	41.2	1.37	3.6
6	Granite	2.592	50.9	1.66	3.4
7	Granite	2.520	58.8	1.69	5.3
8	Chalk	1.504	2.2	1.24	2.0

Table 9. Properties of Rock at White Sands Missile Range Test Sites

Target Rock Type	Core No.	Depth (m)	Natural Porosity (%)	Dry Density (g/cm ³)	Grain Density (g/cm ³)	Unconfined Compressive Strength (MPa)	Modulus of Elasticity (GPa)	Poisson's Ratio	RQD	Remarks
Granite	2A	0.47-0.57	unknown	2.49	unknown	32.77	4.97	0.51	20	Granite, moderately hard, moderately weathered, fractured with up to 1/2 in. of calcareous filling in joints. Dry, gray and pink.
	2A	0.78-1.01	unknown	2.53	unknown	29.07	7.31	0.92		
	2A	1.11-1.27	unknown	2.50	unknown	unknown	11.52	0.17		
Basalt	3	0.00-0.09	28.4	unknown	2.91	30.26	unknown			Basalt, hard, slightly weathered, highly vesicular, moderately fractured with some fractures filled with calcareous material.
	3	0.09-0.21	31.5	2.01	2.93	unknown	5.93	0.14		
	3	0.31-0.52	36.5	unknown	2.96	unknown	13.87	0.19		
Basalt	3	0.52-0.67	unknown	1.91	unknown	21.74	0.14			
	3	1.32-1.49	unknown	2.21	unknown	30.50	13.87	0.19		
	3AN	0.05-0.41	31.0	unknown	2.97	unknown	unknown			Same as core no. 3 except slightly to moderately weathered.
Basalt	3AN	0.46-0.61	28.7	unknown	2.94	unknown	unknown			
	3AS	0.00-0.06	23.7	unknown	2.90	unknown	unknown			
	3AS	0.09-0.22	31.8	unknown	2.89	unknown	unknown			
Limestone	5C	0.00-0.12	unknown	2.63	unknown	82.14	64.72	0.28		
	5C	0.21-0.35	unknown	2.67	unknown	128.26	60.31	0.30		
	5C	1.36-1.49	unknown	2.68	79.54	42.57	0.31			
Sandstone	6	0.14-0.25	unknown	2.60	unknown	146.53	26.84	0.10		
	6	0.39-0.45	unknown	2.58	unknown	unknown	unknown			
	6	1.42-1.49	unknown	2.62	unknown	unknown	unknown			
Shale	7	0.10-0.15	unknown	2.31	unknown	unknown	unknown			
	7	0.24-0.29	unknown	1.84	unknown	unknown	unknown			
	7	0.52-0.57	unknown	2.02	unknown	unknown	unknown			

Table 10. Results of WSMR Scale Rock Fluke Tests

Rock Type	Test No.	Position of Embedded Fluke Base			Time Embedded	Holding Capacity, H (kN)	Displacement at Maximum H (mm)	Embedded Length (cm)	Maximum Embedded Diameter (cm)	Remarks
		Axial Distance Below Target Surface (cm)	Distance Above Crater Bottom (cm)	Axial Tilt of Embedded Fluke (degree from vertical)						
Granite	2A-1	137.3	7.0	6.4	1.3	17 hr 55 min	80.1	2.03	23.72	4.00 All flukes extracted, no apparent damage. Fine rock particles fused over all fluke bodies in thin layer and also concentrated in clumped (up to 5 cm) radial extensions at approximately 5 cm forward of the fluke base.
	-2	137.3	4.0	8.9	1.9	17 hr 52 min	114.6	3.30	23.12	3.93
	-3	137.3	8.0	7.6	3.8	17 hr 52 min	55.2	6.10	21.22	3.74
	-4	137.3	8.0	7.6	3.8	2 hr 58 min	169.1	11.43	21.22	3.74
	-5	137.3	2.0	14.0	5.1	2 hr 52 min	61.4	5.84	19.92	3.60
Basalt	3A-1	137.3	15.0	8.9	2.5	172 days	7.1	1.63	22.52	3.87 Threaded base of fluke damaged, extracted after welding on connecting rod.
	-2	137.3	5.0	11.2	7.6	2 hr 55 min	21.6	9.40	17.42	3.34 Nose of fluke hooked 90 deg.
	-3	137.3	45.0	10.9	2.0	172 days	0.2	0.00	23.02	3.92 Nose of fluke hooked 180 deg, threaded base of fluke damaged.
	-4	137.3	15.0	10.2	0.0	2 hr 30 min	86.8	8.38	25.02	4.06 No damage to fluke.
	-5	137.3	5.0	9.9	0.0	1 hr 02 min	13.1	9.65	25.02	4.06 Piston penetrated 10 cm into basalt (staying in contact with fluke). No fluke damage.

continued

Table 10. Continued

Rock Type	Test No.	Position of Embedded Fluke Base			Time Embedded	Holding Capacity, R (kN)	Displacement at Maximum H (mm)	Embedded Length (cm)	Maximum Embedded Diameter (cm)	Remarks
		Muzzle Velocity (m/sec)	Axial Tilt of Embedded Fluke (degree from vertical)	Distance Below Target Surface (cm)						
Limestone	SC-1	137.3	50.0	7.6	2.5	175 days	38.5	0.86	22.52	3.87
	-2	137.3	0	6.4	0.0	3 hr 43 min	100.1	0.76	25.02	4.06
	-3	106.8	--	--	--	--	--	--	--	--
	-4	137.3	--	--	--	--	--	--	--	--
	-5	137.3	12.5	5.1	0.0	175 days	7.1	19.05	25.02	4.06

continued

Table 10. Continued

Rock Type	Test No.	Muzzle Velocity (m/sec)	Position of Embedded Fluke Base			Time Embedded	Holding Capacity, H (kN)	Displacement at Maximum H (mm)	Embedded Length (cm)	Maximum Embedded Diameter (cm)	Remarks
			Axial Tilt of Embedded Fluke (degree from vertical)	Distance Below Target Surface (cm)	Distance Above Crater Bottom (cm)						
Sandstone	6-1	137.3	22.5	21.6	0.0	17 hr 50 min	4.2	1.27	25.02	4.06	Fluke nose bent 45 deg.
	-2	137.3	6.5	23.6	0.0	17 hr 35 min	4.06	25.02	4.06	4.06	Slight bend to nose.
	-3	137.3	90.0	17.0	2.0	174 days	0.0	23.02	3.92	3.92	Fluke curled up 225 deg.
	-4	137.3	--	--	--	--	--	--	--	--	Base damaged, connection welded on. Pulled out by hand.
	-5	106.8	90.0	24.8	2.0	173 days	0.2	0.00	23.02	3.92	Fluke nose hooked 180 deg. Base damaged, connection welded on. Pulled out by hand.
Shale	7-1	106.8	15.0	35.6	-25.4	7 hr 00 min	8.2	10.67	25.02	4.06	All flukes extracted, no damage to flukes or pistons.
	-2	106.8	5.0	25.4	-15.2	2 hr 13 min	5.2	13.97	25.02	4.06	As in granite tests layer of crushed rock adhered to entire body of fluke with some increase in thickness toward the base. Pistons remained seated on flukes after embedment.
	-3	106.8	45.0	24.1	-16.5	2 hr 34 min	6.0	8.89	25.02	4.06	
	-4	106.8	15.0	32.4	-20.3	1 hr 55 min	8.7	5.59	25.02	4.06	
	-5	137.3	5.0	41.3	-20.3	1 hr 00 min	7.4	9.14	25.02	4.06	

Table 11. Standard Deviation of WSMR Test Data

Type Rock	Test	Holding Capacity, H (kN)	Statistics by Rock Type			Statistics for All Tests	
			\bar{H} (kN)	σ (kN)	Value of H 83% Confident of Exceeding (kN)	\bar{H} (kN)	σ (kN)
Granite	1-1	80.1	96.08	46.9	49.18	54.97	50.05
	1-2	114.6					
	1-3	55.2					
	1-4	169.1					
	1-5	61.4					
Basalt	3A-1	7.10	32.15	36.92	(0)	4.92	4.92
	3A-2	21.6					
	3A-4	86.8					
	3A-5	13.1					
Limestone	5C-1	38.5	48.57	47.31	1.26	1.26	1.26
	5C-2	100.1					
	5C-5	7.1					
Sandstone	6-1	4.2	7.45	4.60	2.85	2.85	2.85
	6-2	10.7					

Table 12. Results of Simple Regression Performed
on the Independent Variables

Independent Variable	Form of Best Fit Equation	A	B	Standard Error of Estimate	r
μ	$H = A \mu$	138.78		38.62	0.669
μ	$H = A + B \log \mu$	109.35	44.56	41.32	0.679
E	$H = A + B/E$	13.51	436.86	47.79	0.528
R	$H = A + B/R$	0.77	16.61	47.81	0.527
σ	$H = A + B \sigma$	81.30	-0.43	51.58	0.399
1-p	$H = A + B \log (1-p)$	64.11	86.12	53.68	0.299
ρ	$H = A + B/\rho$	146.52	-219.09	54.99	0.211
A_s	$H = A + B A_s$	104.89	-0.67	55.63	0.149
D	$H = A + B D$	177.51	-31.30	55.69	0.143
L	$H = A + B L$	118.00	-2.74	55.79	0.129

Table 13. Results of Empirical Holding Capacity Equation Development
for Embedment Anchors in Rock Seafloors

Trial No.	Independent Variables	Range of Percent Error		Standard Error of Estimate, S	95% Confidence Interval $\pm 1.96S$	Correlation Coefficient, r	Sample Size, N
		+	-				
1	$\sigma, \sigma^2, \sigma^3$	687	61	47.97	94.02	0.453	16
2	ρ, ρ^2	1,360	68	47.32	92.75	0.402	16
3	E, E^2	605	134	43.65	85.55	0.536	16
4	σ, ρ, E, μ, R	583	63	46.62	91.32	0.683	14
5	σ, ρ, E, μ	583	63	43.92	86.08	0.683	14
6	σ, ρ, E	583	63	41.70	81.73	0.683	14
7	σ, ρ, μ	578	63	41.70	81.73	0.683	14
8	σ, ρ	672	80	40.00	78.40	0.678	14
9	E, μ	544	69	40.22	78.83	0.673	14
10	σ, E, μ	583	63	41.70	81.73	0.683	14
11	$\log \sigma, \log \rho, \log E, \log \mu, \log R$	324	76	49.10	96.24	0.639	14
12	$D, L, \sigma, \rho, R/100, 1-p$	629	51	48.64	95.33	0.701	14
13	D, L, σ, ρ, E, R	650	51	48.41	94.88	0.704	14
14	D, L, σ, ρ, E	648	53	41.02	80.40	0.718	16
15	D, L, σ, ρ	749	80	39.43	77.28	0.712	16
15a	D, L, σ, ρ	746	84	43.03	84.34	0.699	14

continued

Table 13. Continued

Trial No.	Independent Variables	Range of Percent Error		Standard Error of Estimate, S	95% Confidence Interval $\pm 1.96S$	Correlation Coefficient, r	Sample Size, N
		+	-				
16	D, L, E, μ	583	64	43.95	86.14	0.683	14
17	D^2 , L, σ , ρ	724	88	40.03	78.46	0.701	16
18	D, L, σ^2 , ρ^2	905	178	40.91	80.18	0.685	16
19	D^2 , L, σ^2 , ρ^2	872	184	41.40	81.14	0.676	16
20	D^4 , L, σ^3 , ρ^3 , E^3 , R	630	51	48.59	95.24	0.702	14
21	D^4 , L, σ^3 , ρ^3 , E^3	626	54	40.91	80.18	0.718	16
22	D^2 , L, σ^3 , ρ^3 , E^3	621	56	40.97	80.30	0.719	16
23	D^4 , L, σ^3 , ρ^2 , E^2 , R	628	52	48.72	95.49	0.701	14
24	D^4 , L, σ^3 , ρ^2 , E^2	627	54	41.00	80.36	0.718	16
25	D^6 , D^2 , L, σ^3 , ρ^2 , E^2 , R	695	48	51.99	101.90	0.709	14
26	D^6 , D^2 , L, σ^3 , ρ^2 , E^2	679	70	42.81	83.91	0.725	16
26a	D^6 , D^2 , L, σ^3 , ρ^2 , E^2	700	47	48.05	94.18	0.710	14
27	D^3 , D, σ , E	844	57	51.93	101.78	0.382	16
28	D^6 , L^2 , L, σ^3 , ρ^2 , E^2	664	69	42.79	83.87	0.725	16
28a	D^6 , L^2 , L, σ^3 , ρ^2 , E^2	656	52	48.65	95.35	0.701	14
29	D^8 , L^8 , σ^6 , ρ^6 , E^6 , R^3	687	48	48.26	94.59	0.707	14
30	D^3 , L^3 , σ^2 , ρ^2 , E^2 , R^3	673	48	48.26	94.59	0.707	14
31	m , v^2 , σ^2 , ρ^2 , E^2 , R^3	582	63	49.84	97.69	0.683	14

continued

Table 13. Continued

Trial No.	Independent Variables	Range of Percent Error		Standard Error of Estimate, S	95% Confidence Interval, $\pm 1.96S$	Correlation Coefficient, r	Sample Size, N
		+	-				
32	$m, v^2, \sigma^3, \rho^3, E^2$	583	64	42.02	82.36	0.701	16
33	m, v^2, σ^3, ρ^3	915	160	43.24	84.75	0.639	16
34	m, v^2, σ, ρ	662	85	40.94	80.24	0.685	16
35	$\log E, -\log \mu, 3 \log D, \log L, (1/2) \log [(D^2/4) + L^2]$	378	76	50.12	98.24	0.619	14
36	$\log E, -\log \mu, 3 \log D, \log L, (1/2) \log [(D^2/4) + L^2], \log (R/100)$	413	72	52.45	102.80	0.639	14
37	$\log E, -\log \mu, 3 \log D, \log L, (1/2) \log [(D^2/4) + L^2], \log (R/100), \log (1-p)$	414	72	56.73	111.19	0.638	14
38	$\log E, -\log \mu, 3 \log D, \log L, (1/2) \log [(D^2/4) + L^2], -\log z$	359	77	53.86	105.57	0.613	14
39	$\log (E/\mu), \log (D^2L), \log [D (D^2/4) + L^2]$	267	84	45.81	87.79	0.596	14
40	$\log E, \log \mu, \log D, \log L, \log [(D^2/4) + L^2], \log R$	412	72	52.46	102.82	0.639	14
41	$D^6, D^2, L^3, L, E, \mu, R/100, 1-p$	721	44	54.87	107.55	0.733	14
42	$D^6, D^2, L^3, L, \sigma^3, \rho^2, E^2$	919	100	57.35	112.41	0.628	14
43	$H/KE = f(m)$					0.669	14

Table 14. Results of Applying Equations Developed From Scale-Model Tests Directly to 20K Rock Fluke

Trial Equation No.	Equation	Granite	Basalt	Limestone	Sandstone	Remarks
26	$H = f(D^6, D^2, L, \sigma^3, \rho^2, E^2)$	246 MN	246 MN	246 MN	246 MN	2nd highest r
32	$H = f(m, v^2, \sigma^3, \rho^3, E^2)$	1.26 MN	1.19 MN	1.21 MN	1.17 MN	$f(m, v^2)$ instead of $f(D, L)$
34	$H = f(m, v^2, \sigma, \rho)$	94.1 kN	31.7 kN	56.7 kN	4.02 kN	lower S than (32)
43	$H = 1/2(mv^2)(1.96 \times 10^{-3})(\mu)$	1.78 MN	43N kN	750 kN	250 kN	highest r

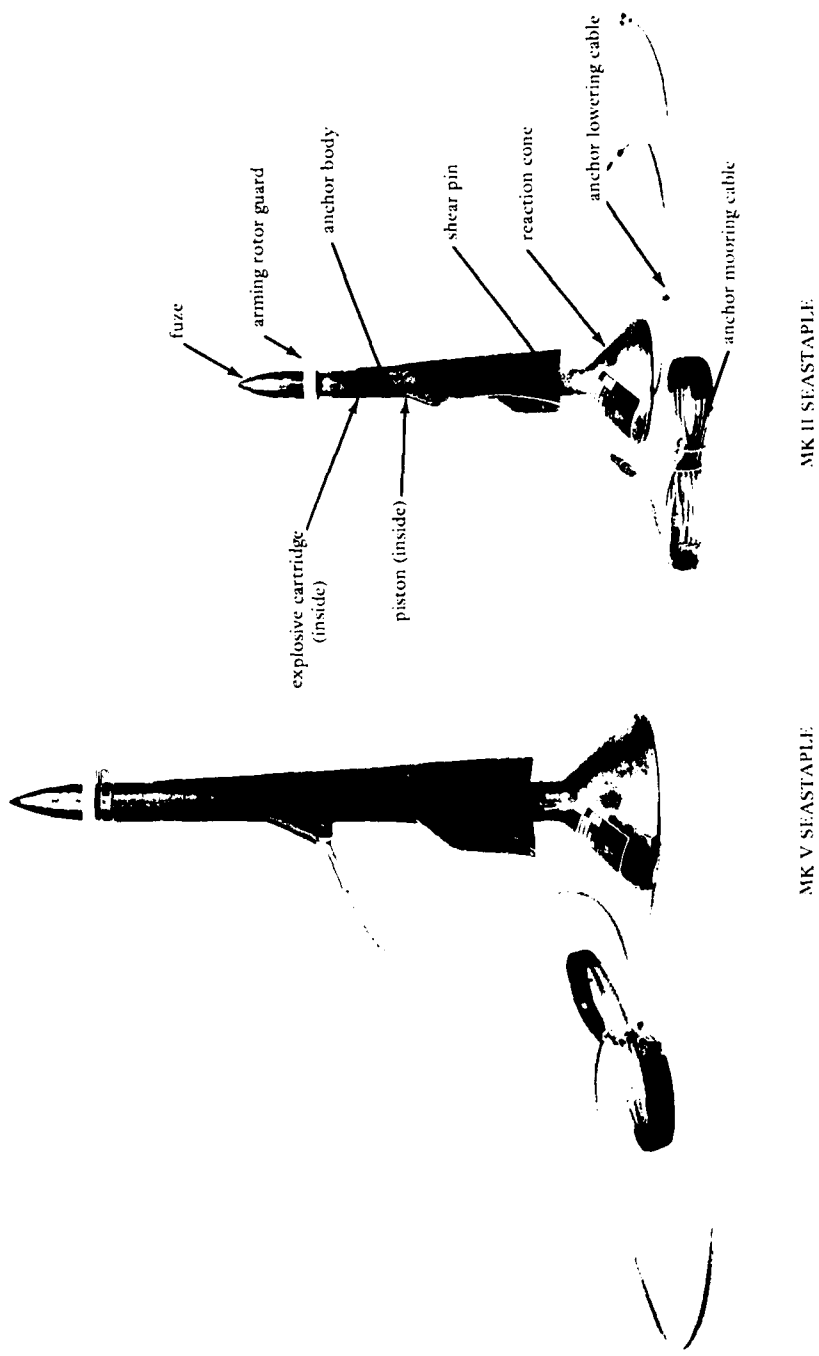


Figure 1. SEASTAPLE explosive embedment anchors.

MK V SEASTAPLE

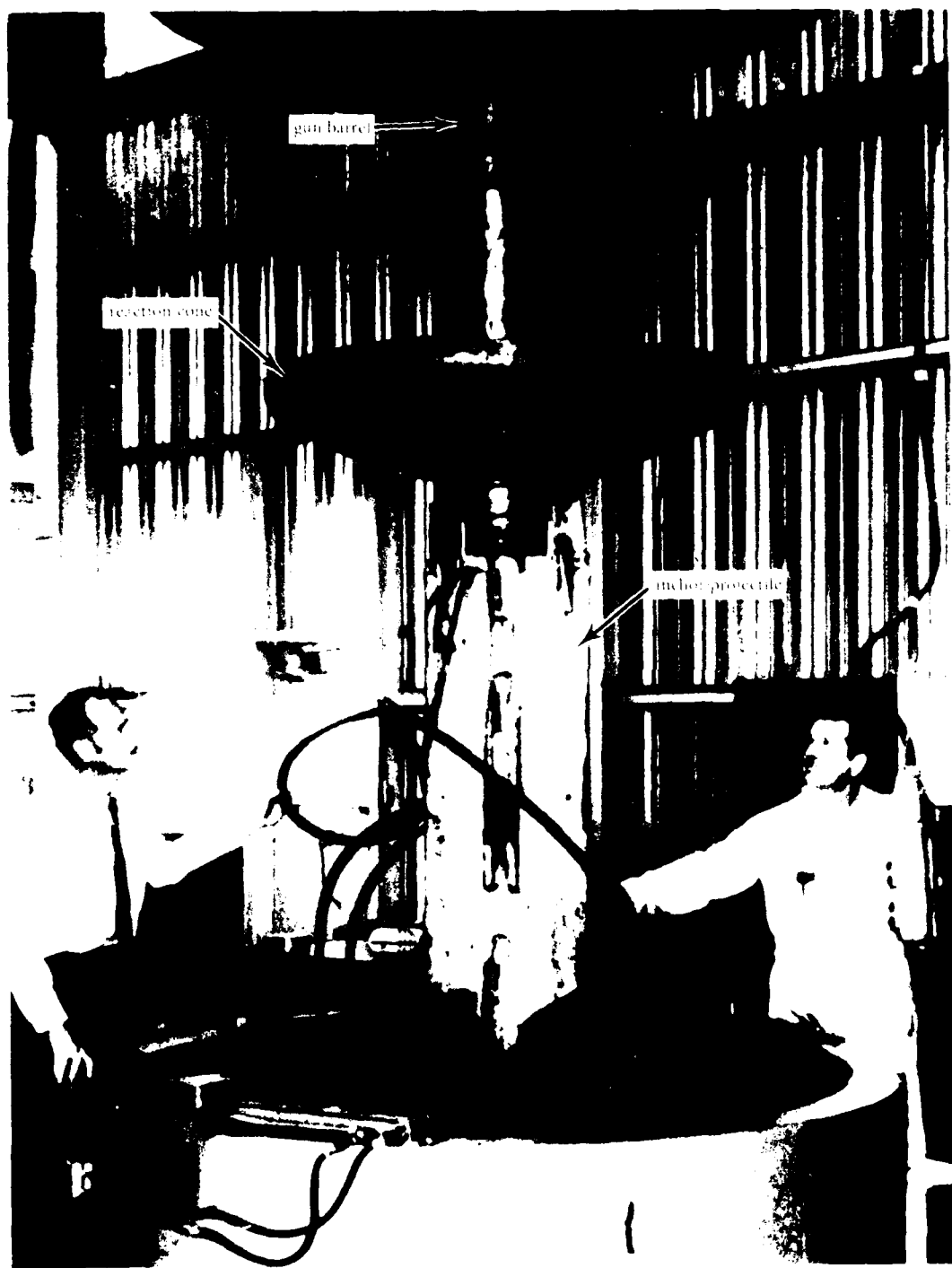


Figure 2a. MERDC 50-K explosive anchor.

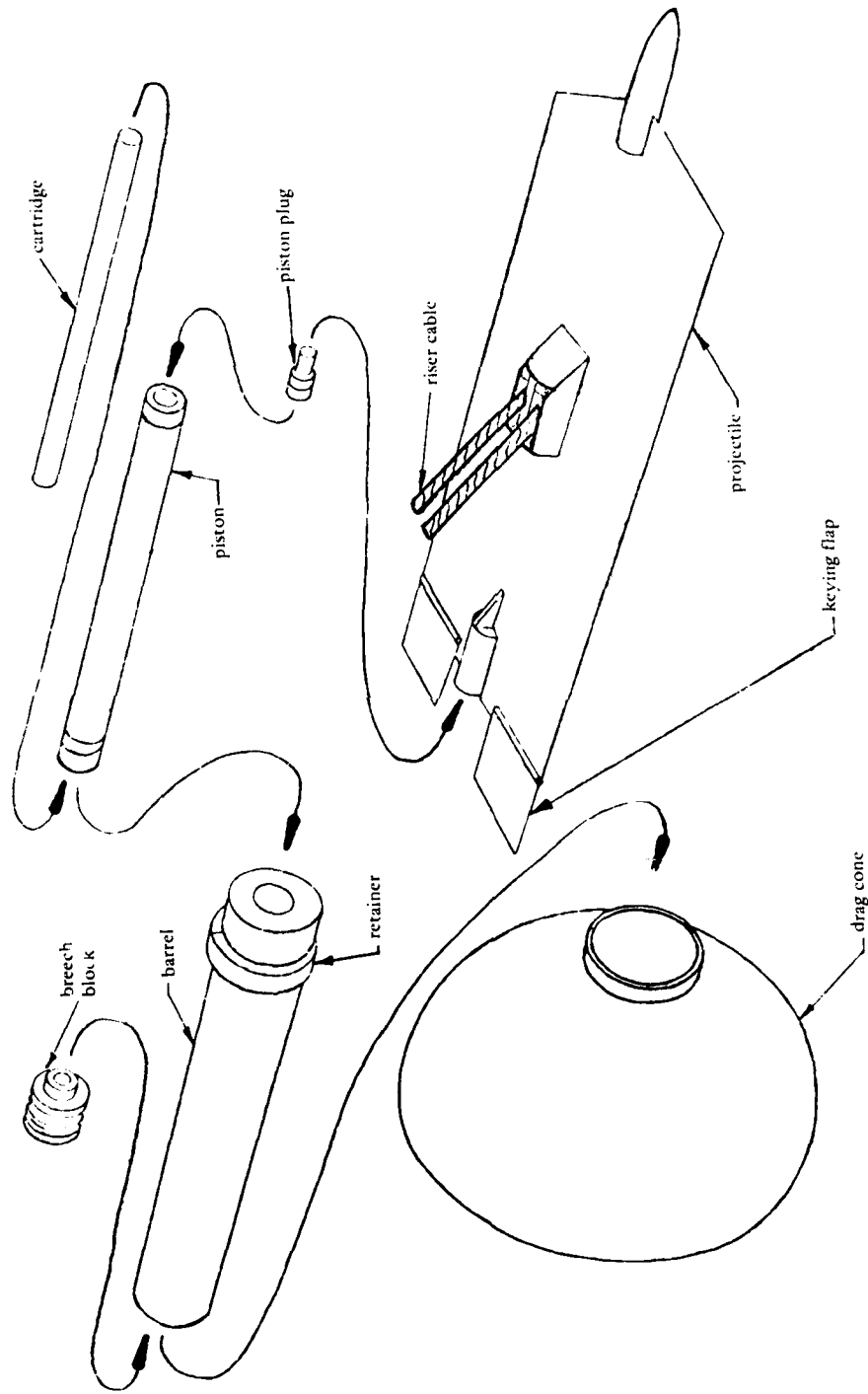


Figure 2b. Schematic of US Army MERDC XM-200 explosive anchor.

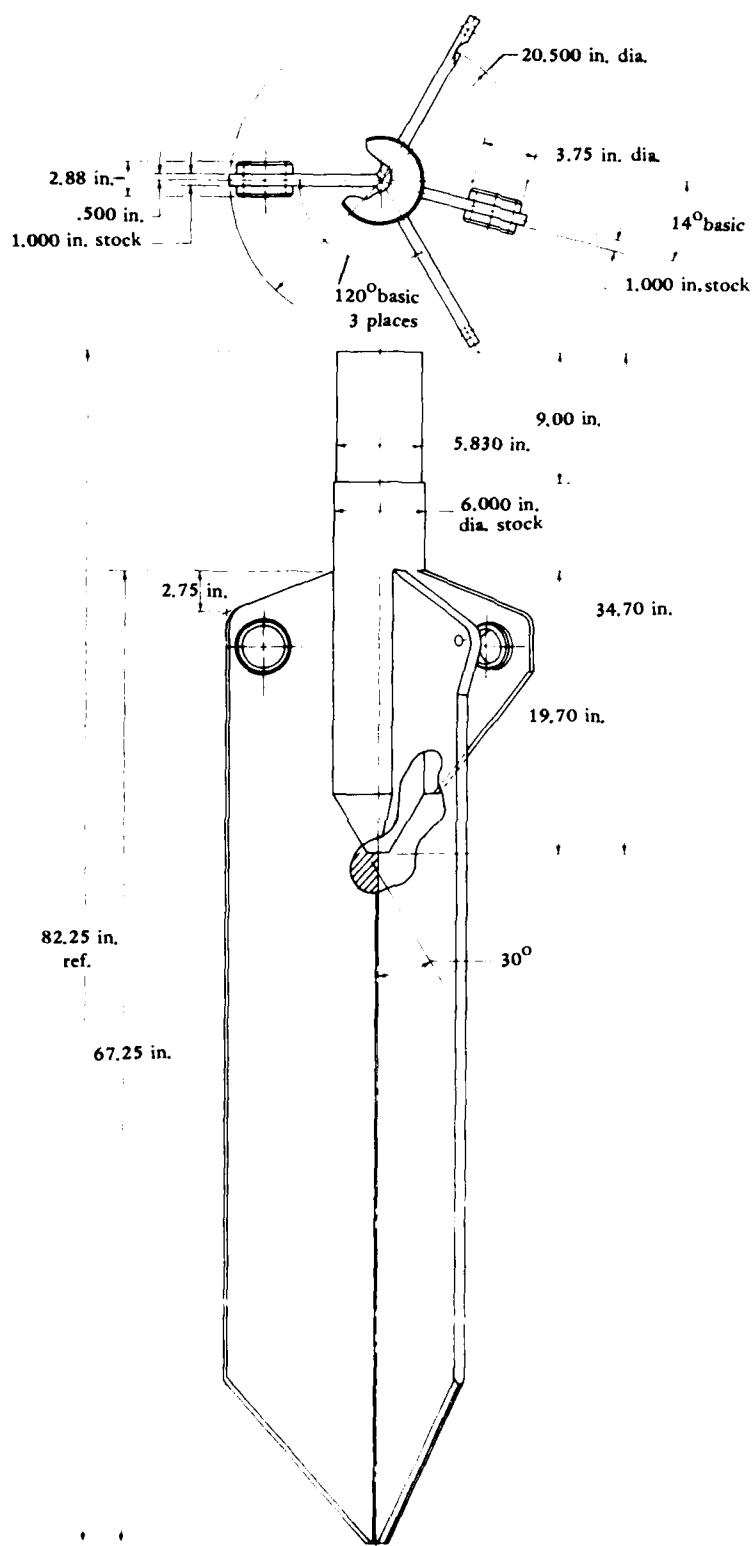


Figure 3a. Original SUPSALV coral fluke (Coral 1).

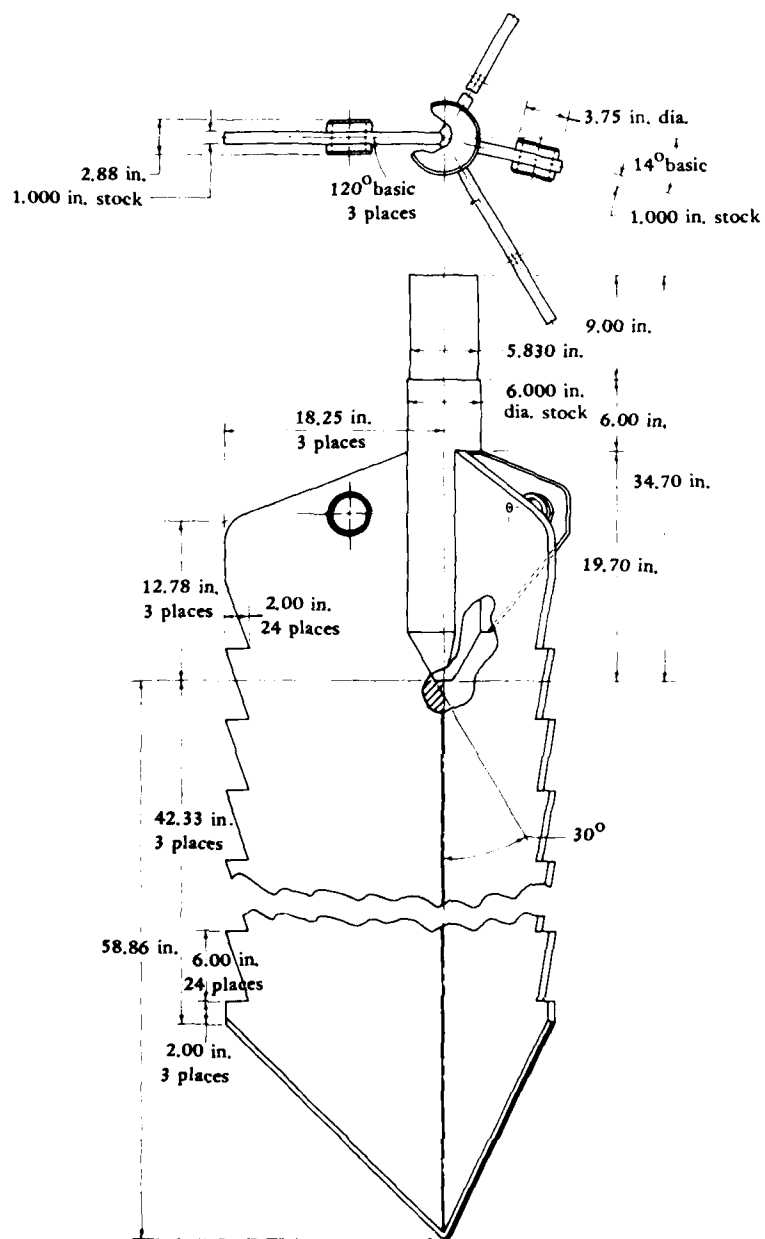


Figure 3b. Modified SUPSALV coral fluke (Coral 2).

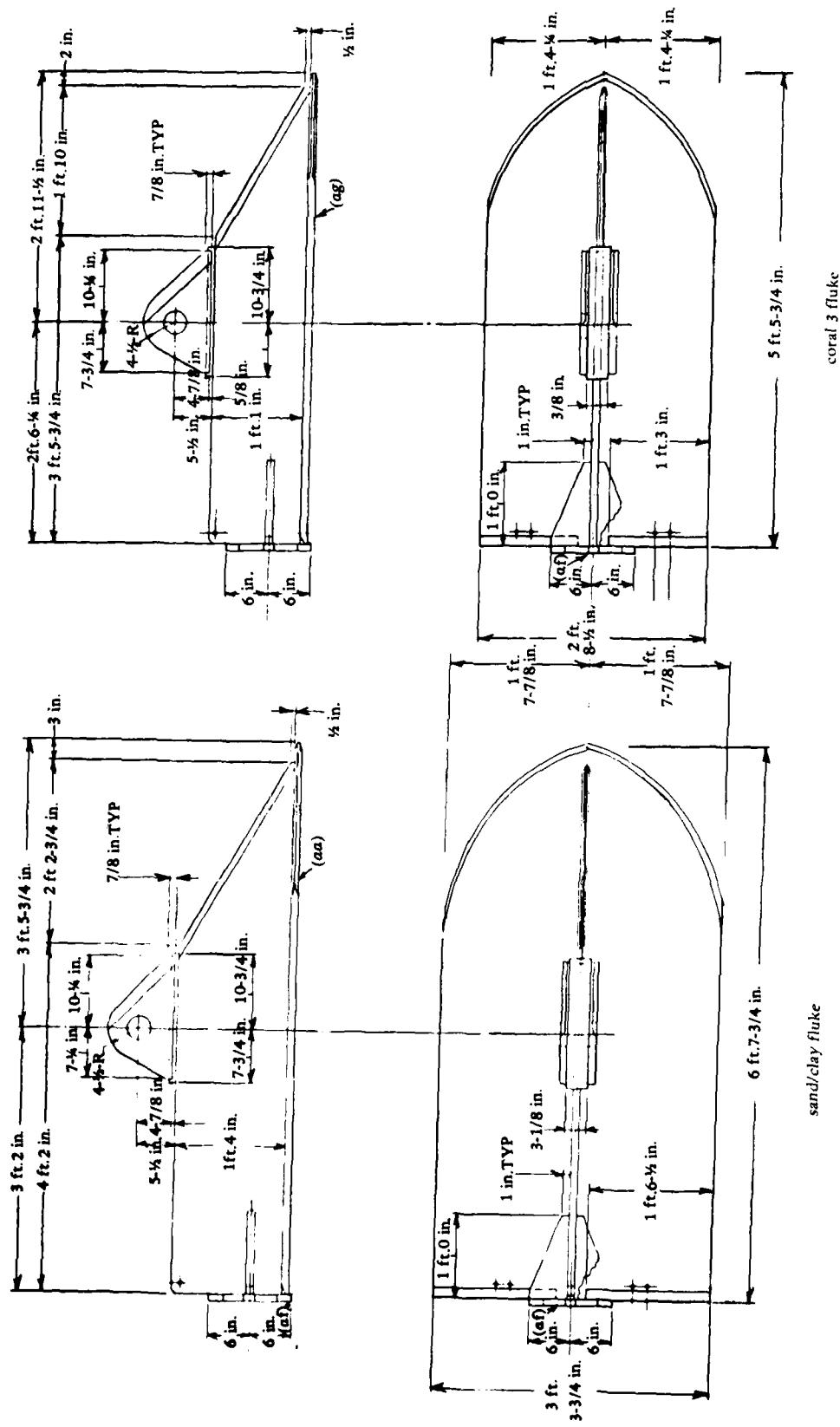


Figure 4a. 100K coral anchors used at Diego Garcia.

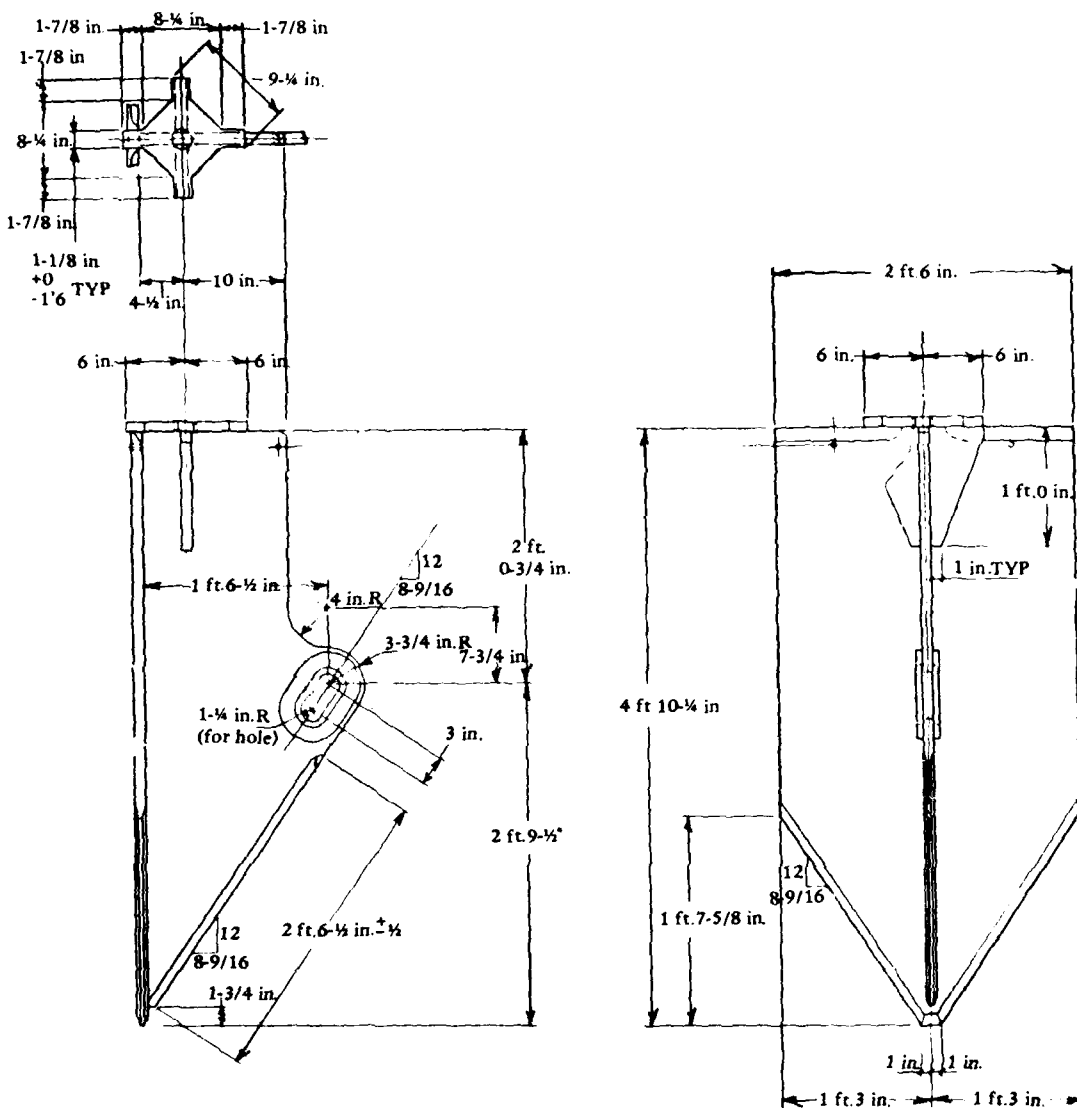


Figure 4b. 100K coral anchor used at Argus Island (Coral 4).

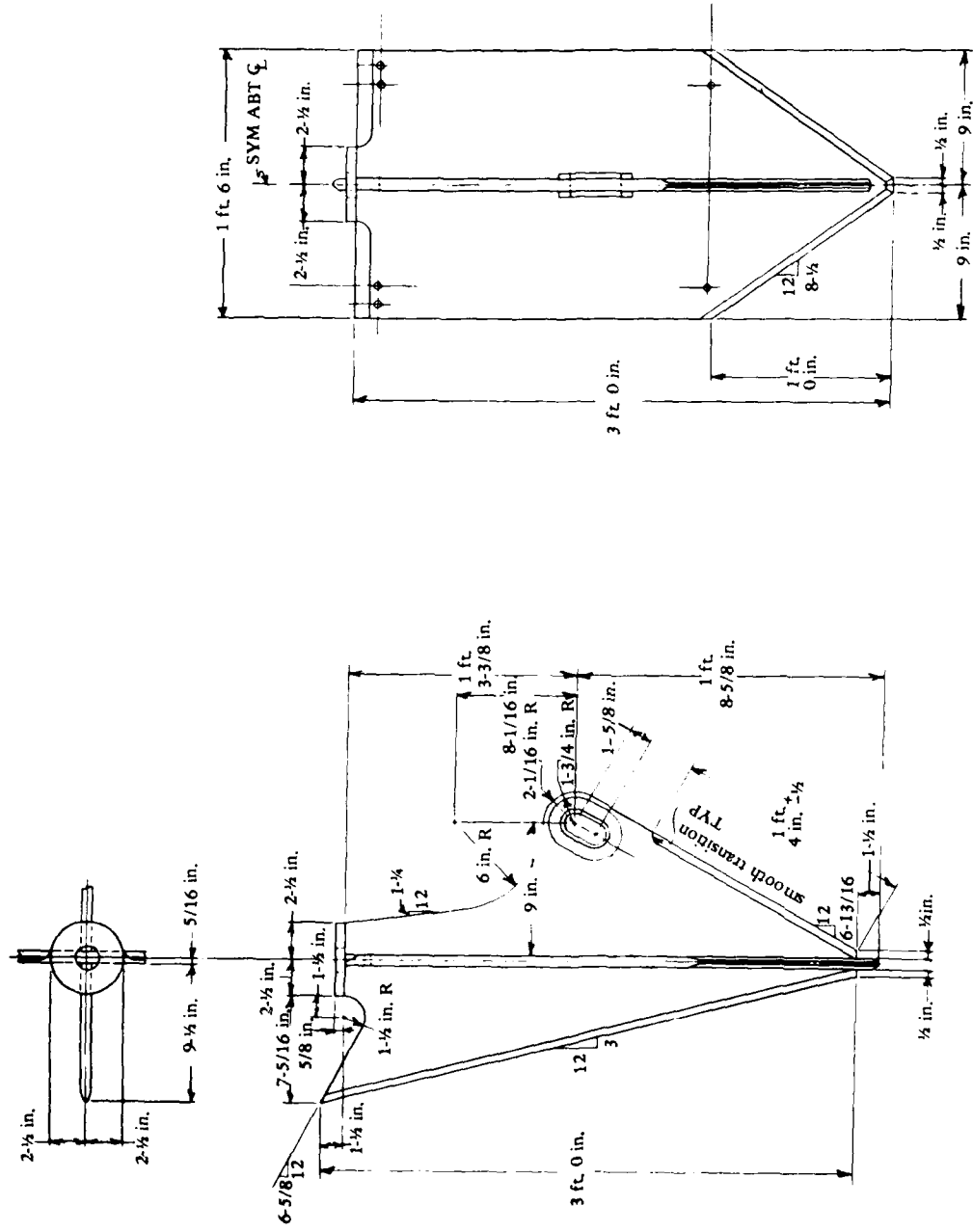


Figure 5. CFI 20K coral anchor fluke used at BARSTUR.

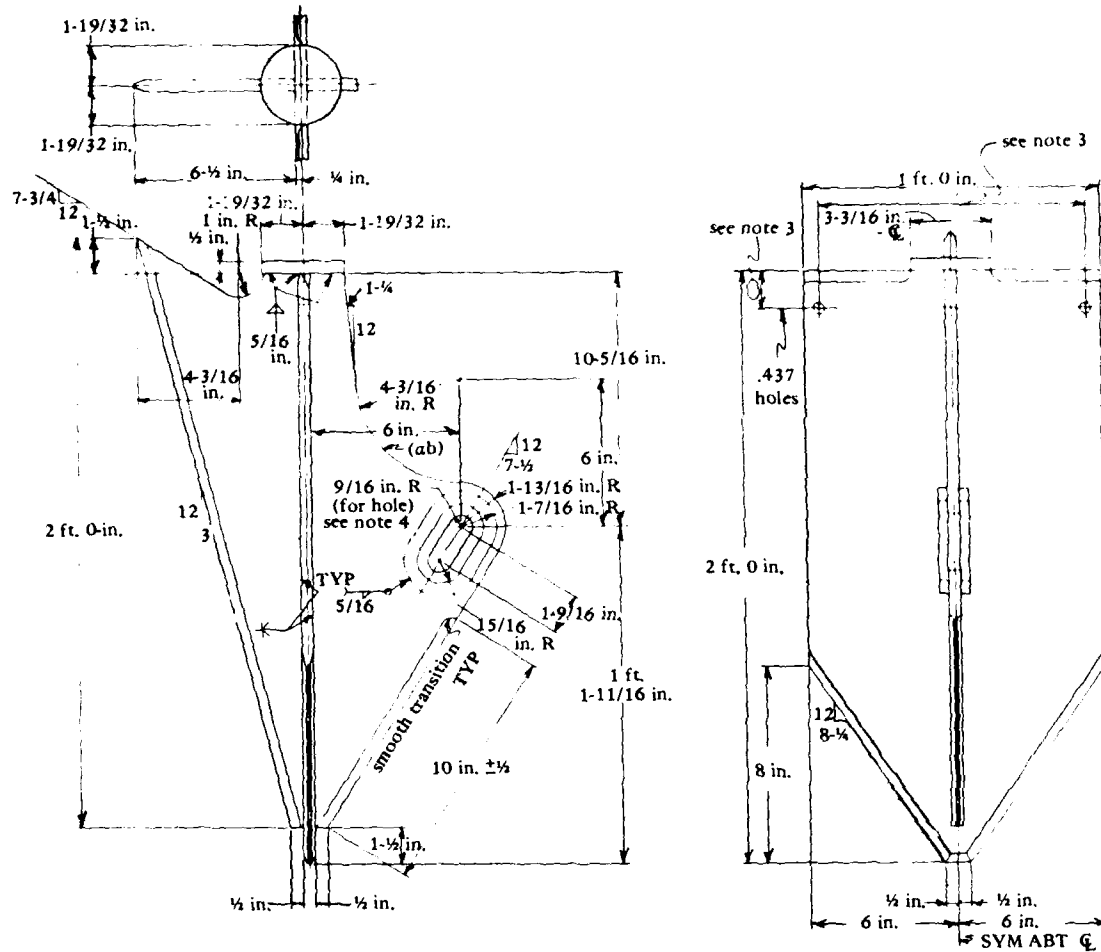


Figure 6. CEL 10K coral fluke used at Barbers Point.

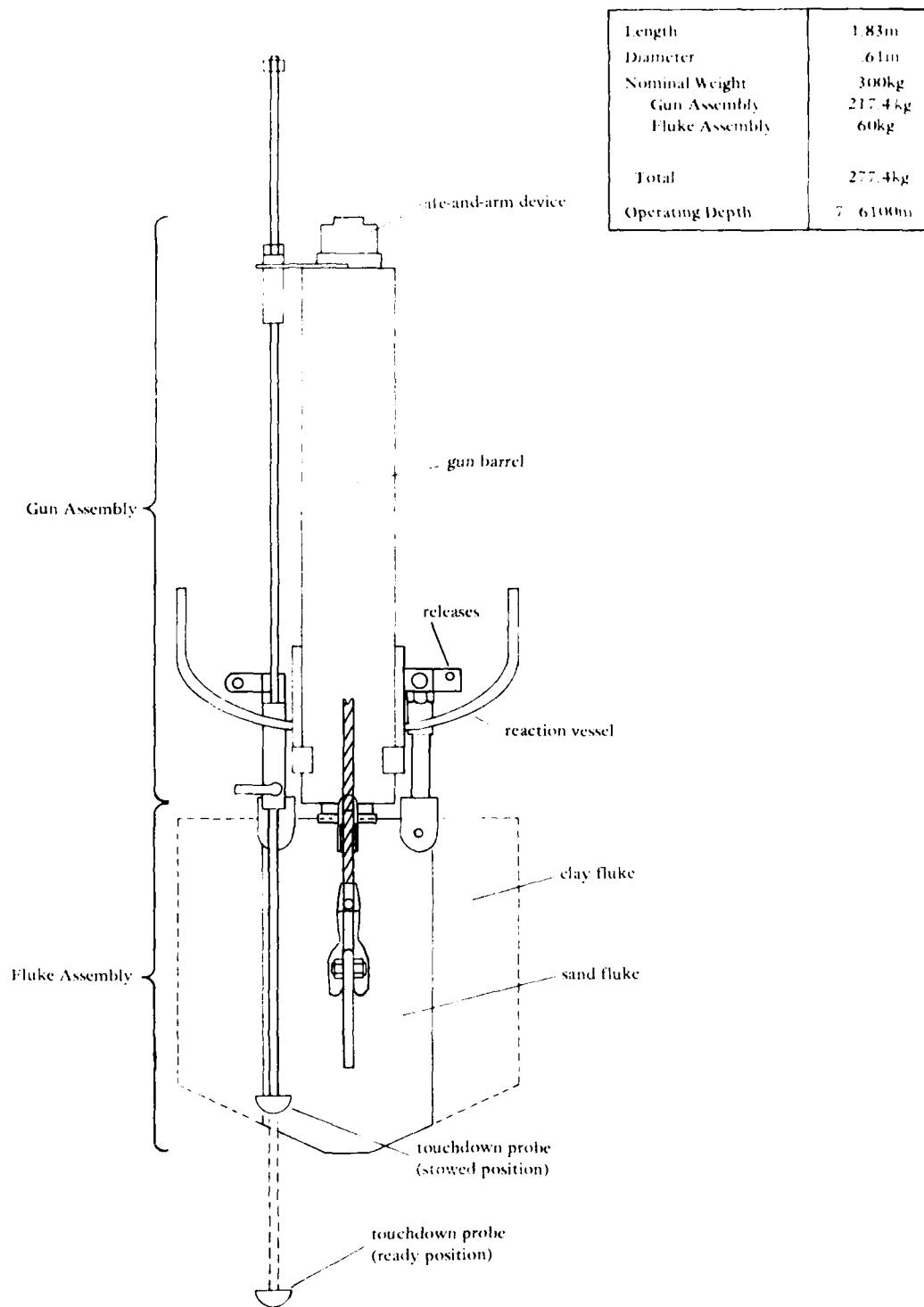


Figure 7. Schematic of the CEL 10K propellant-actuated anchor.



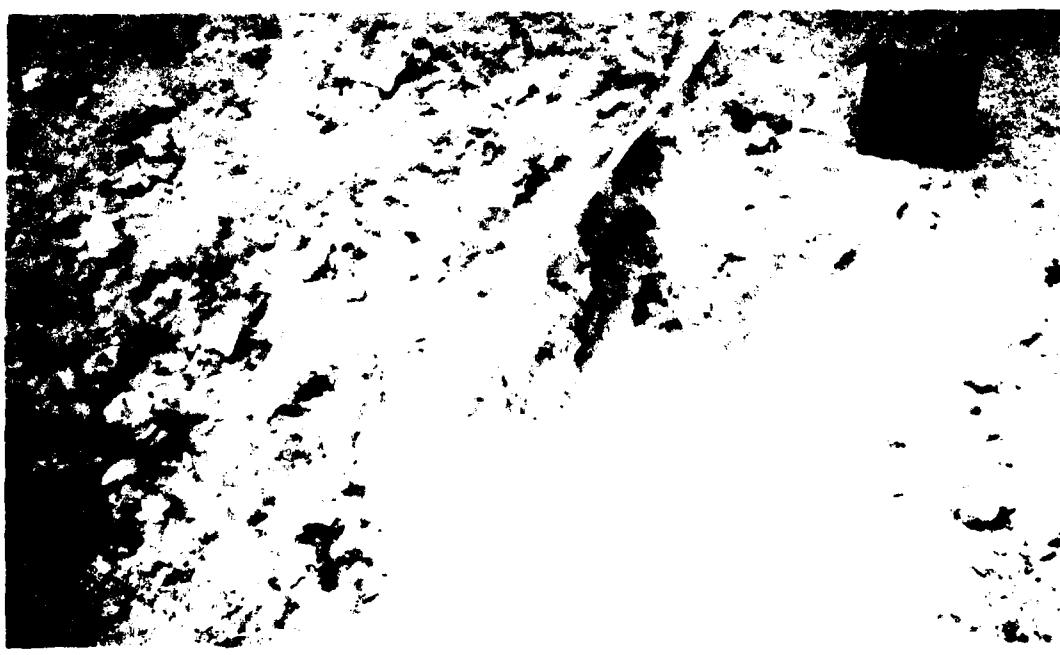
Figure 8. 10K coral fluke embedded in coral seafloor off Barbers Point, Oahu.



Figure 9. Same 10K coral fluke (see Figure 8) after loading to failure of the wire rope downhaul.



a. Before.



b. After.

Figure 10. Before and after load testing an embedded 10K cori' flake

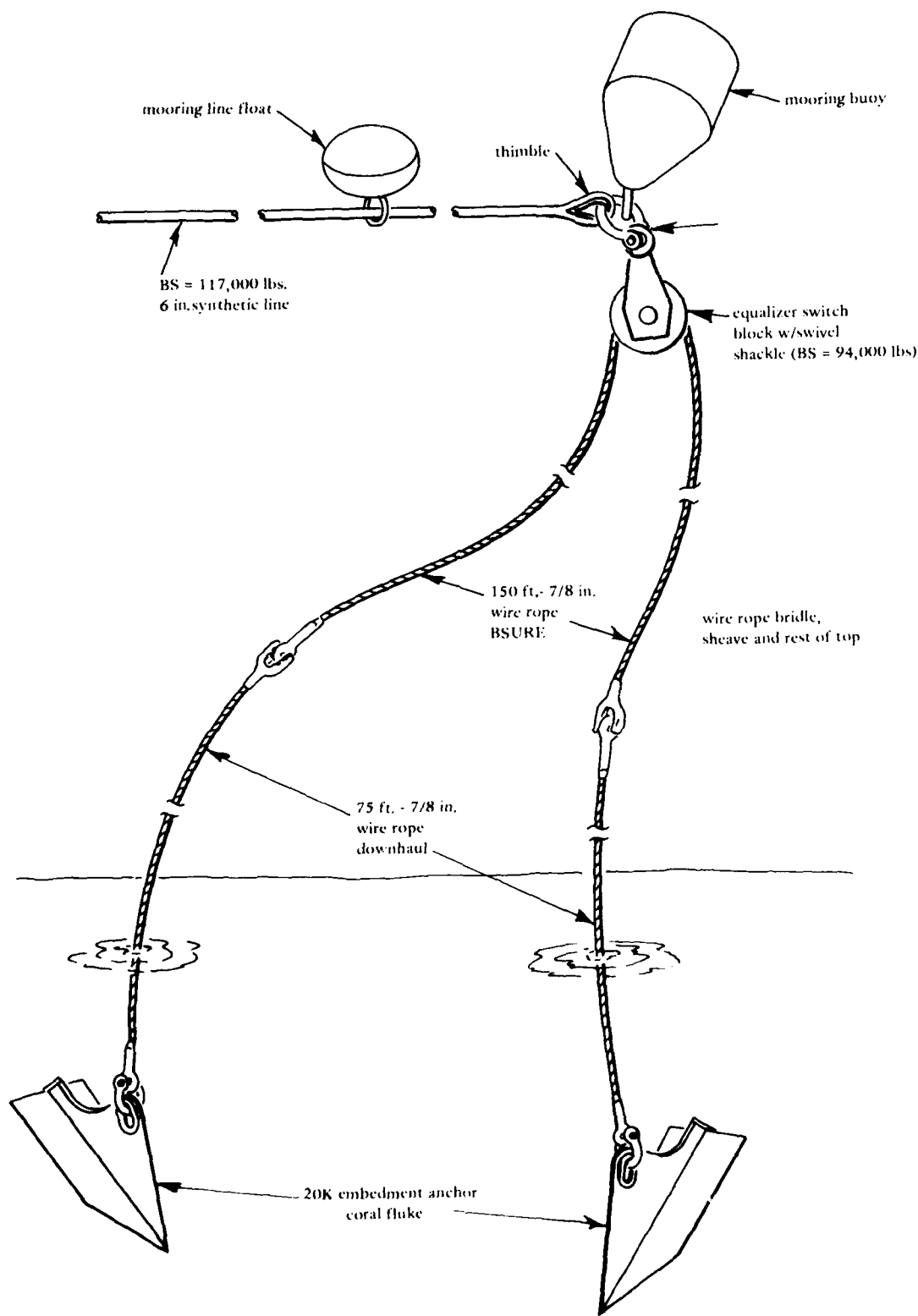


Figure 11. BSURE mooring leg.

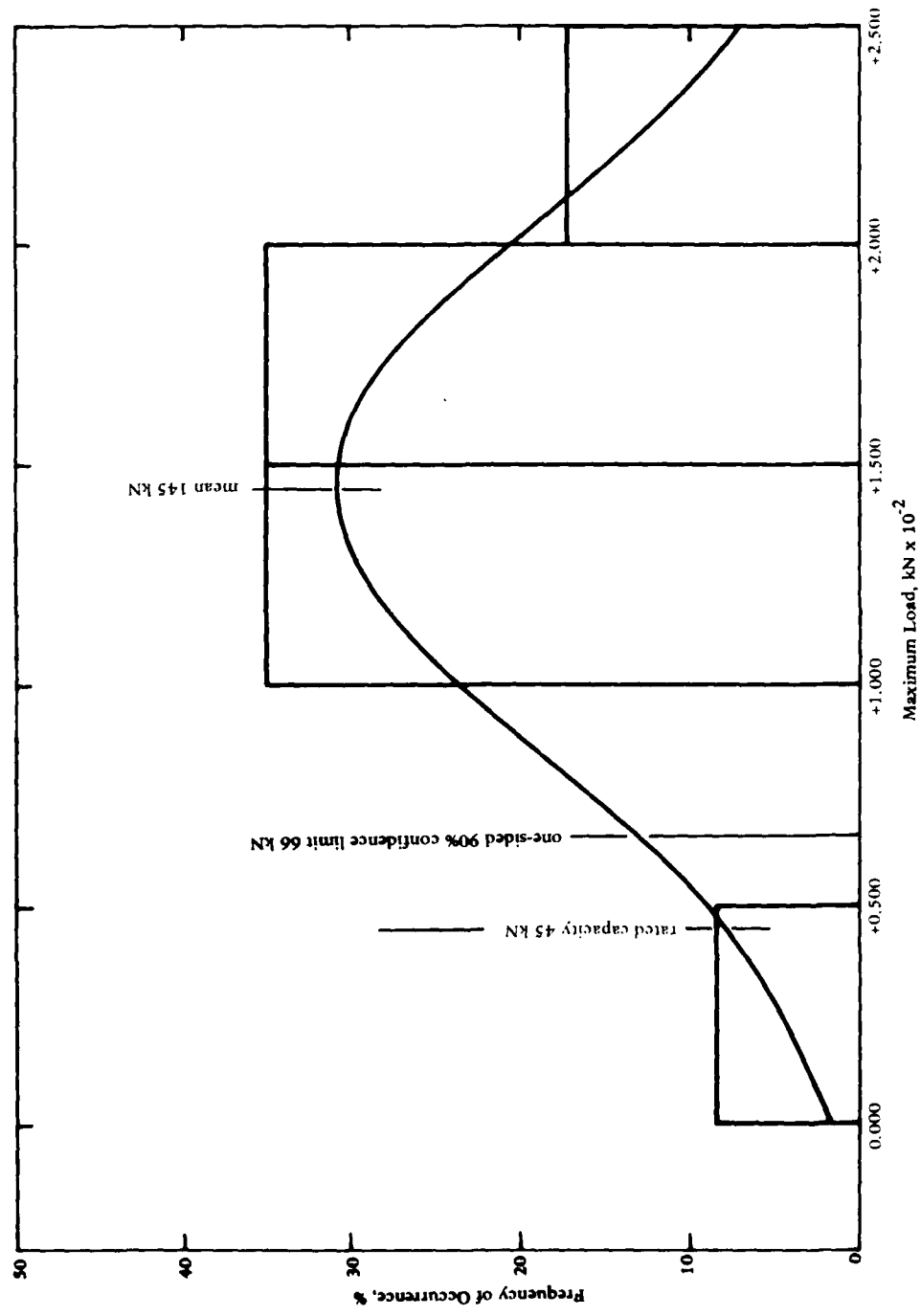


Figure 12. Distribution of data from Barbers Point tests.

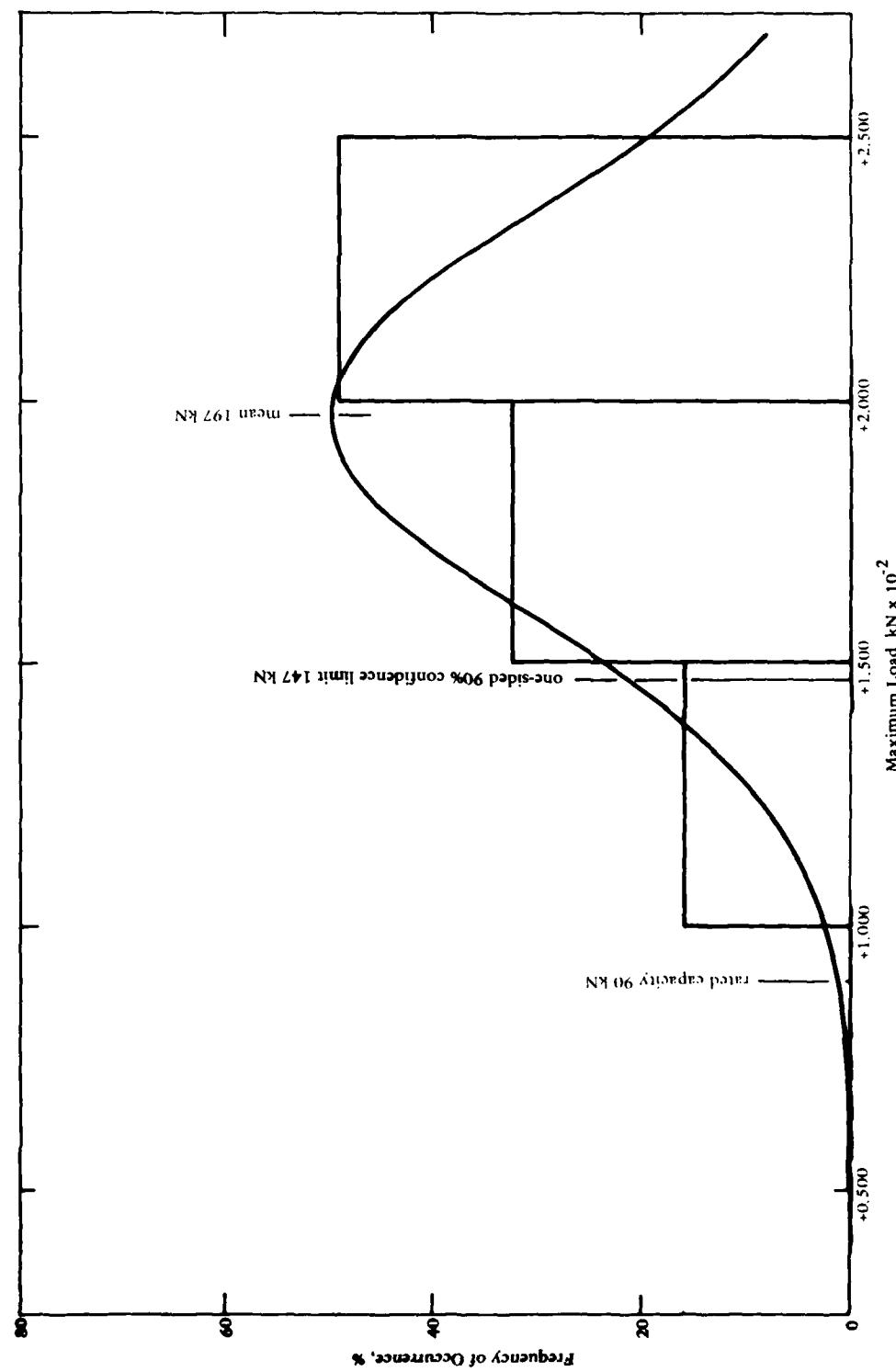


Figure 13. Distribution of data from BARSICR tests.

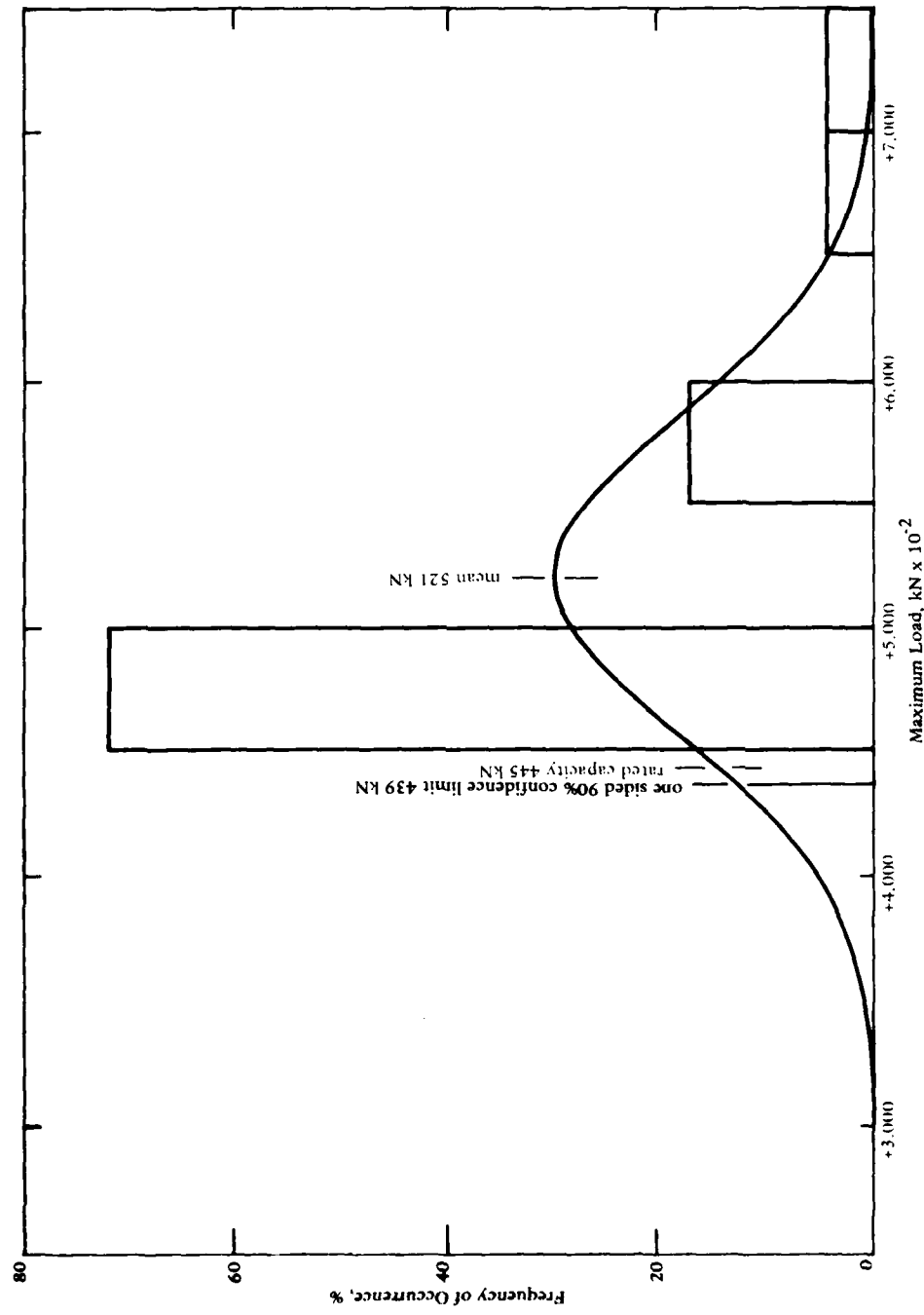


Figure 14. Distribution of data from proof-loadings at Diego Garcia and Argus Island.

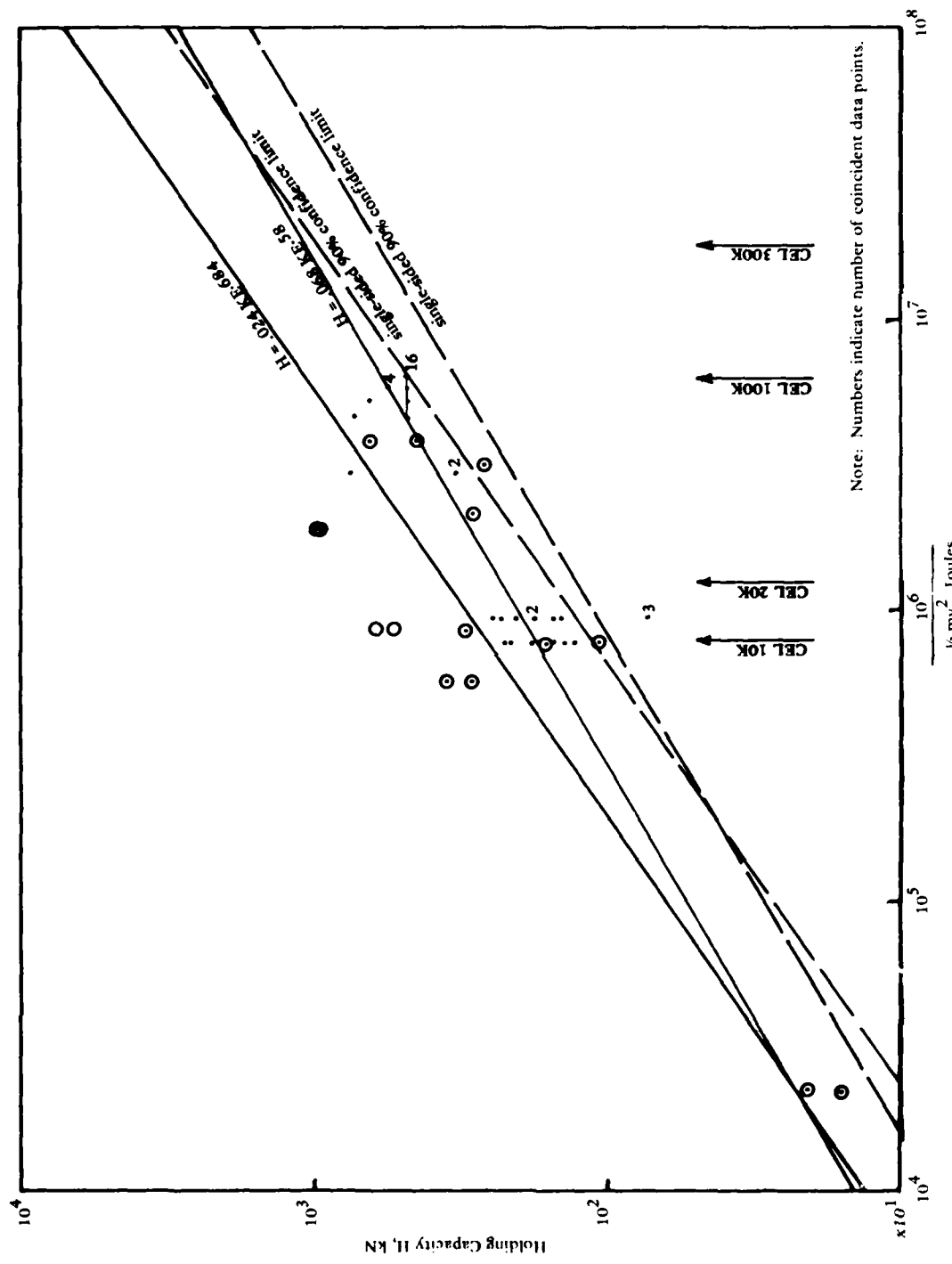


Figure 15. Holding capacities in coral plotted versus fluke kinetic energy.

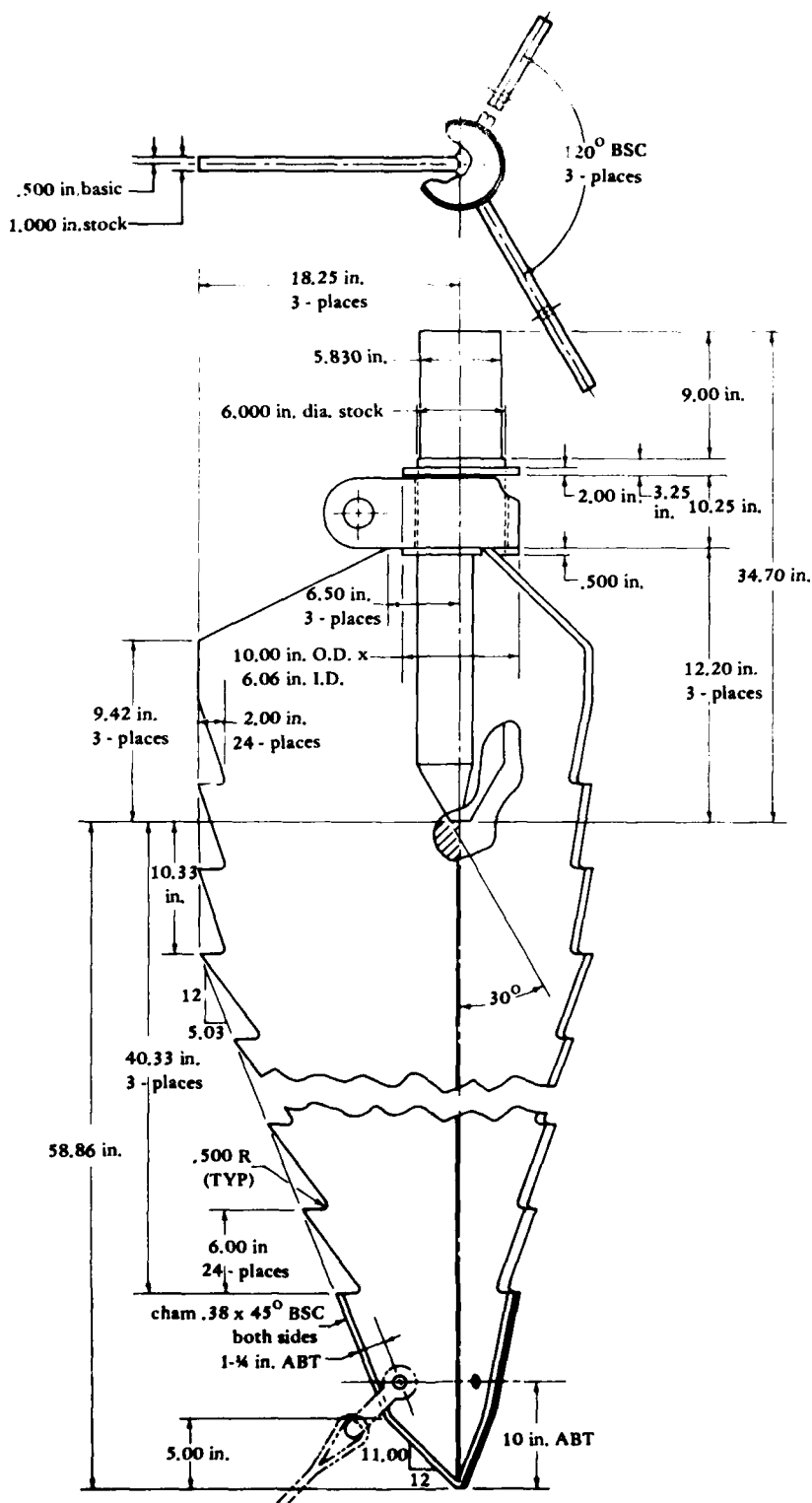


Figure 16. SUPSALV rock fluke.

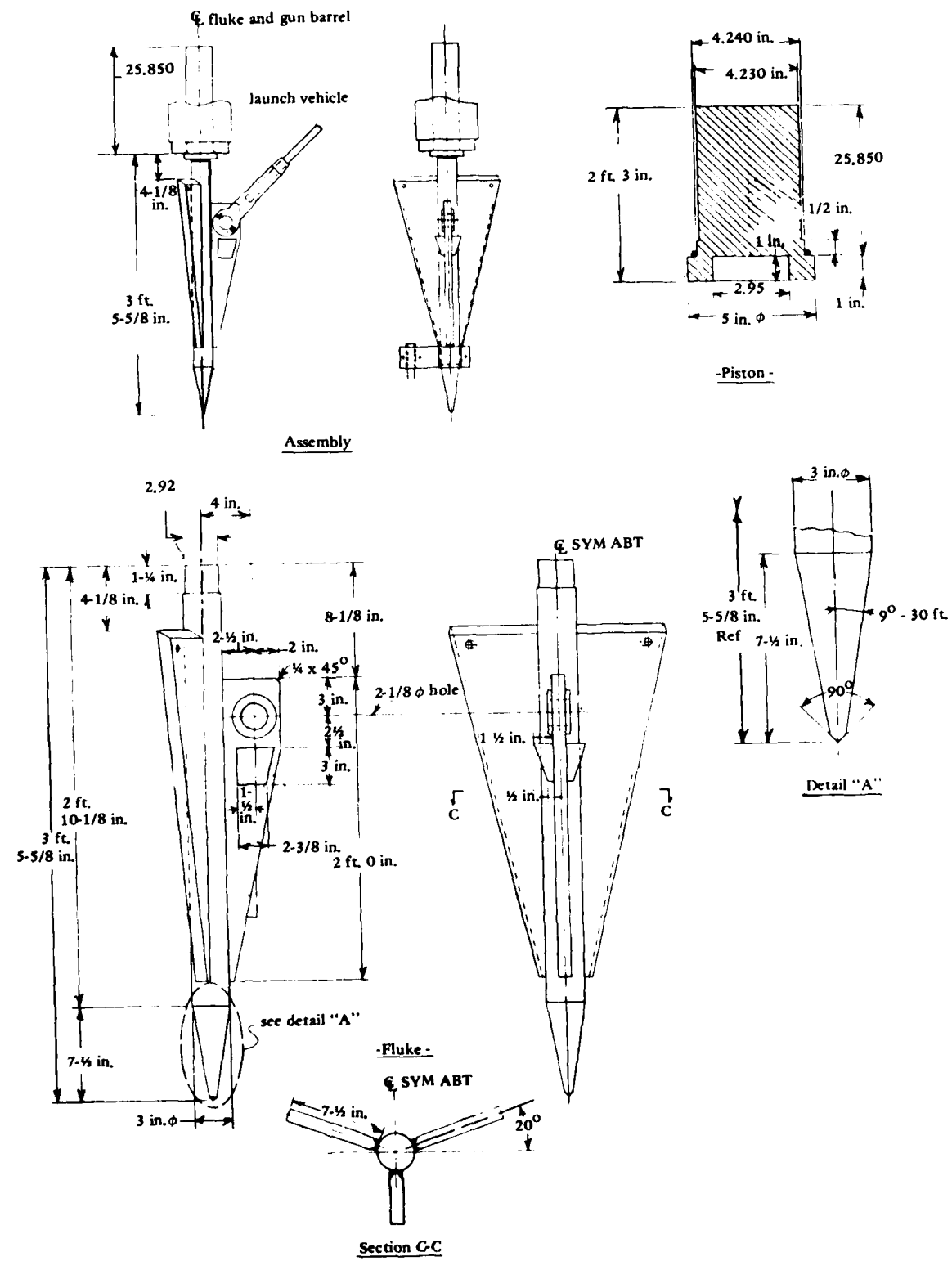


Figure 17. CEL 20K rock fluke.

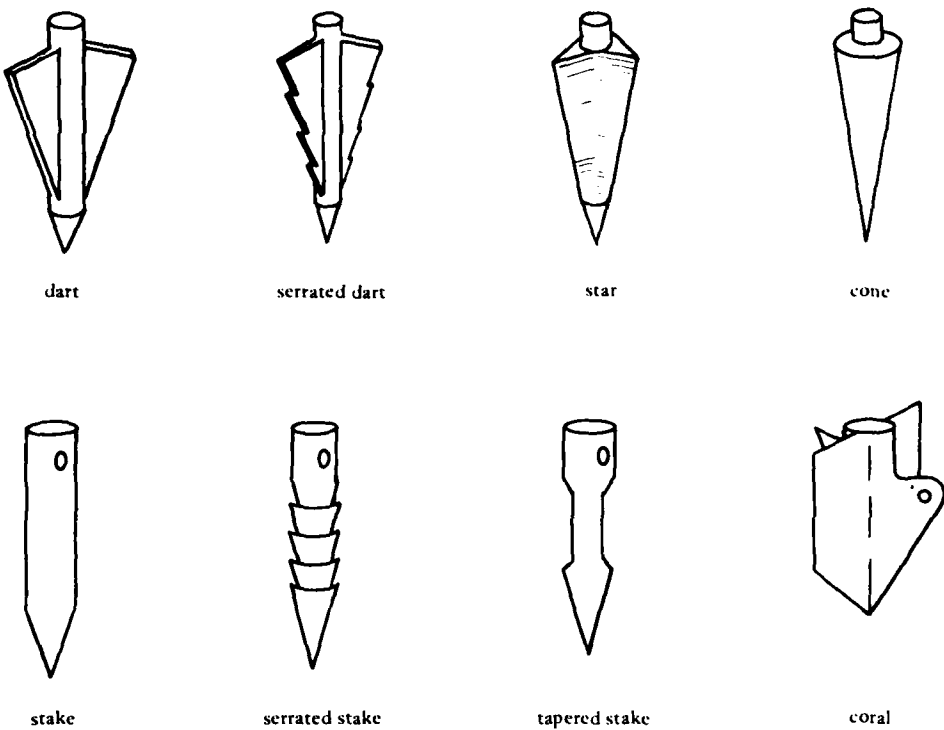


Figure 18. Fluke shapes tested at NWC, China Lake.

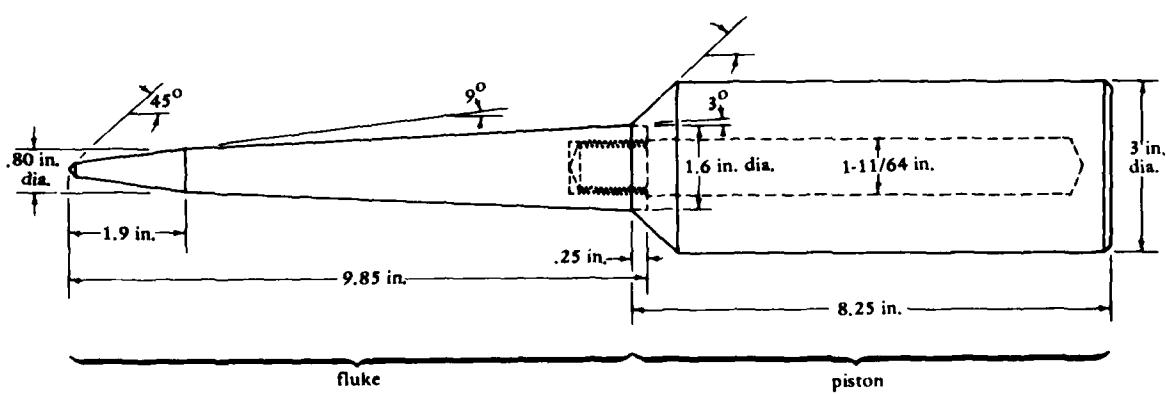


Figure 19. Rock fluke and piston configuration used in all WSMR tests.

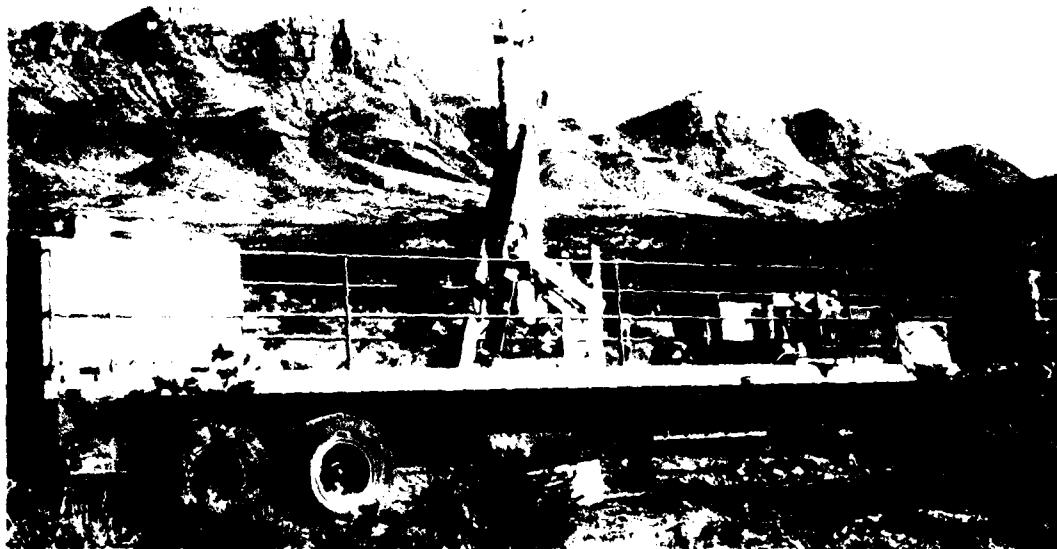


Figure 20. Sandia Laboratories' pneumatic launching system.

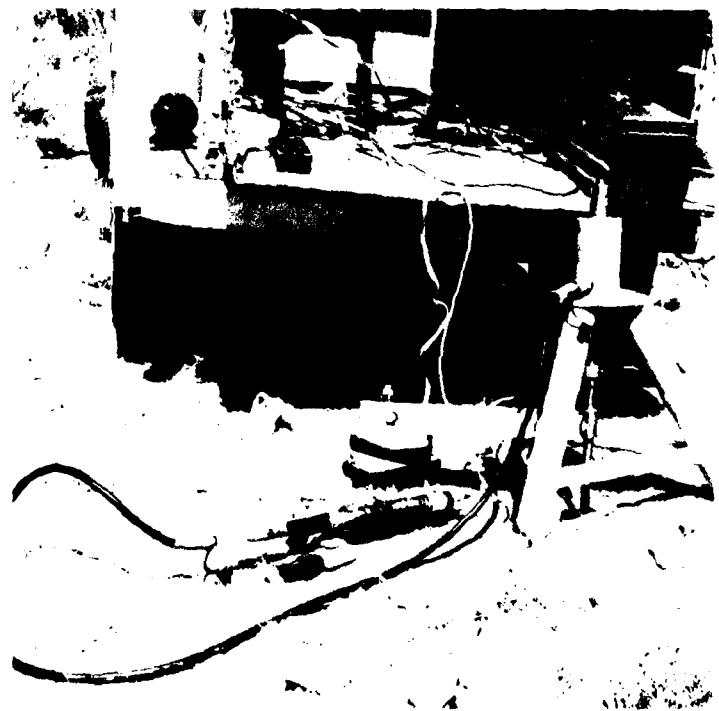


Figure 21. Hydraulic extractor and load displacement measurement equipment used for WSMR tests.

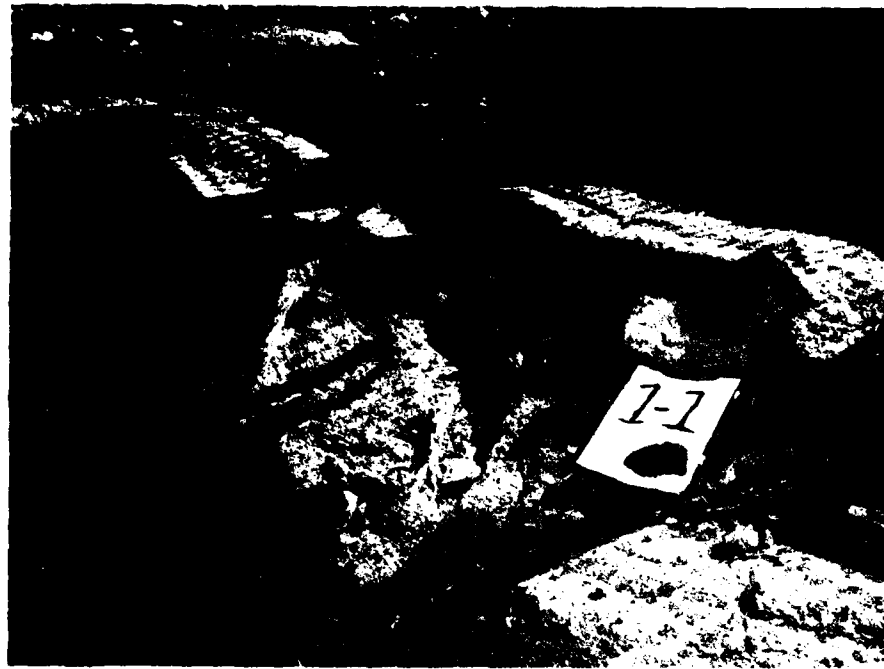


Figure 22a. Typical embedment of scale rock fluke in granite.

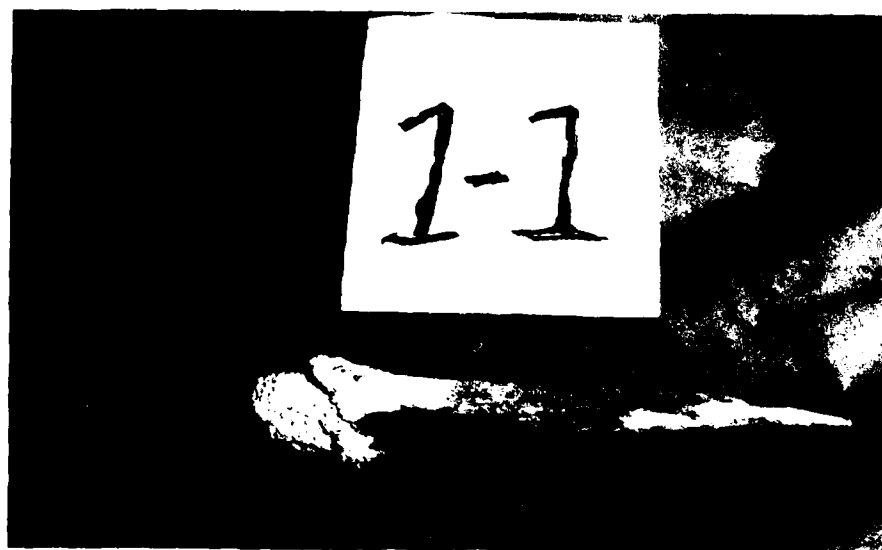


Figure 22b. Condition of fluke following extraction from granite.



Figure 23a. Typical embayment of scale rock tholeiite in vesicular basalt.

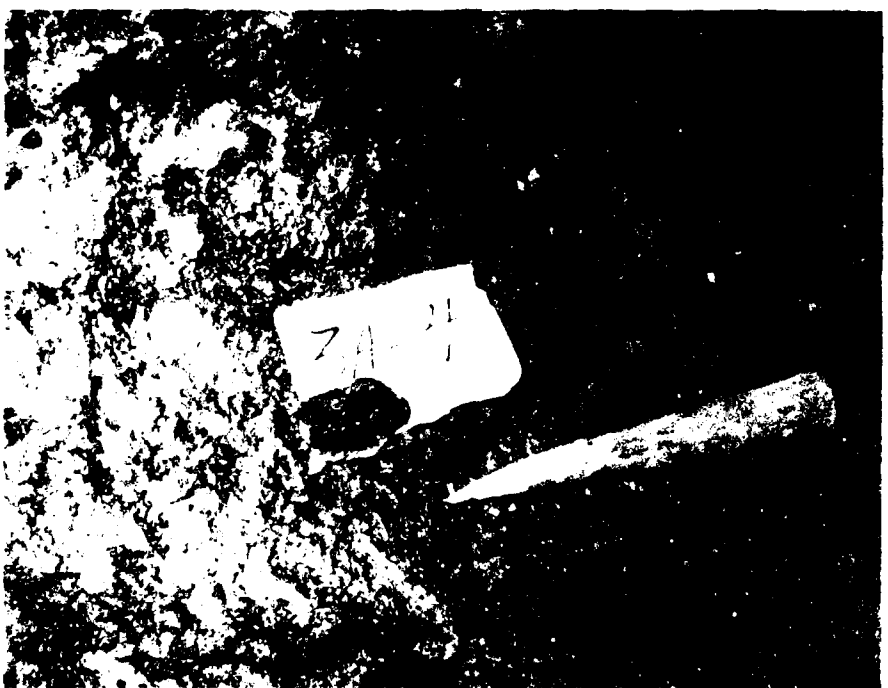


Figure 23b. Another view of the same sample as in Figure 23a, showing a thin probe.

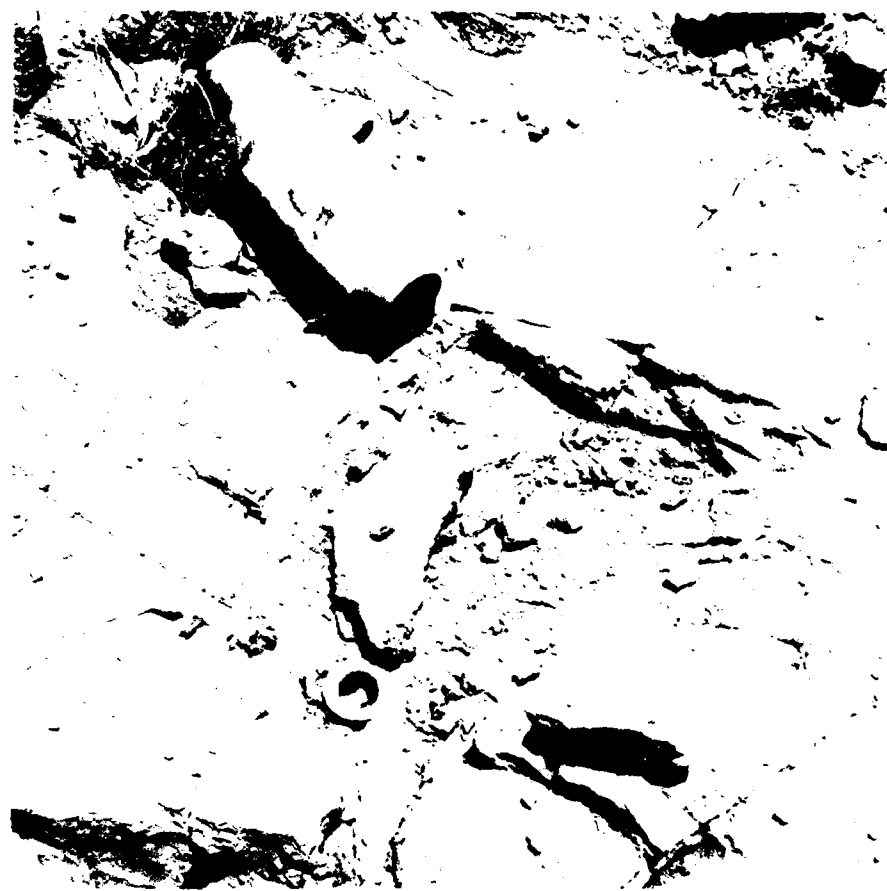


Figure 24a. Appearance of a successful embedment in limestone.



Figure 24b. Condition of fluke and target after extraction



Figure 25a. Typical condition of target following embedment in sandstone.



Figure 25b. Condition of thule after extraction from sandstone.



Figure 26a. Rock fluke embedded in shale after removing piston and clearing away shattered rock.



Figure 26b. Typical condition of fluke and piston after extraction from shale.

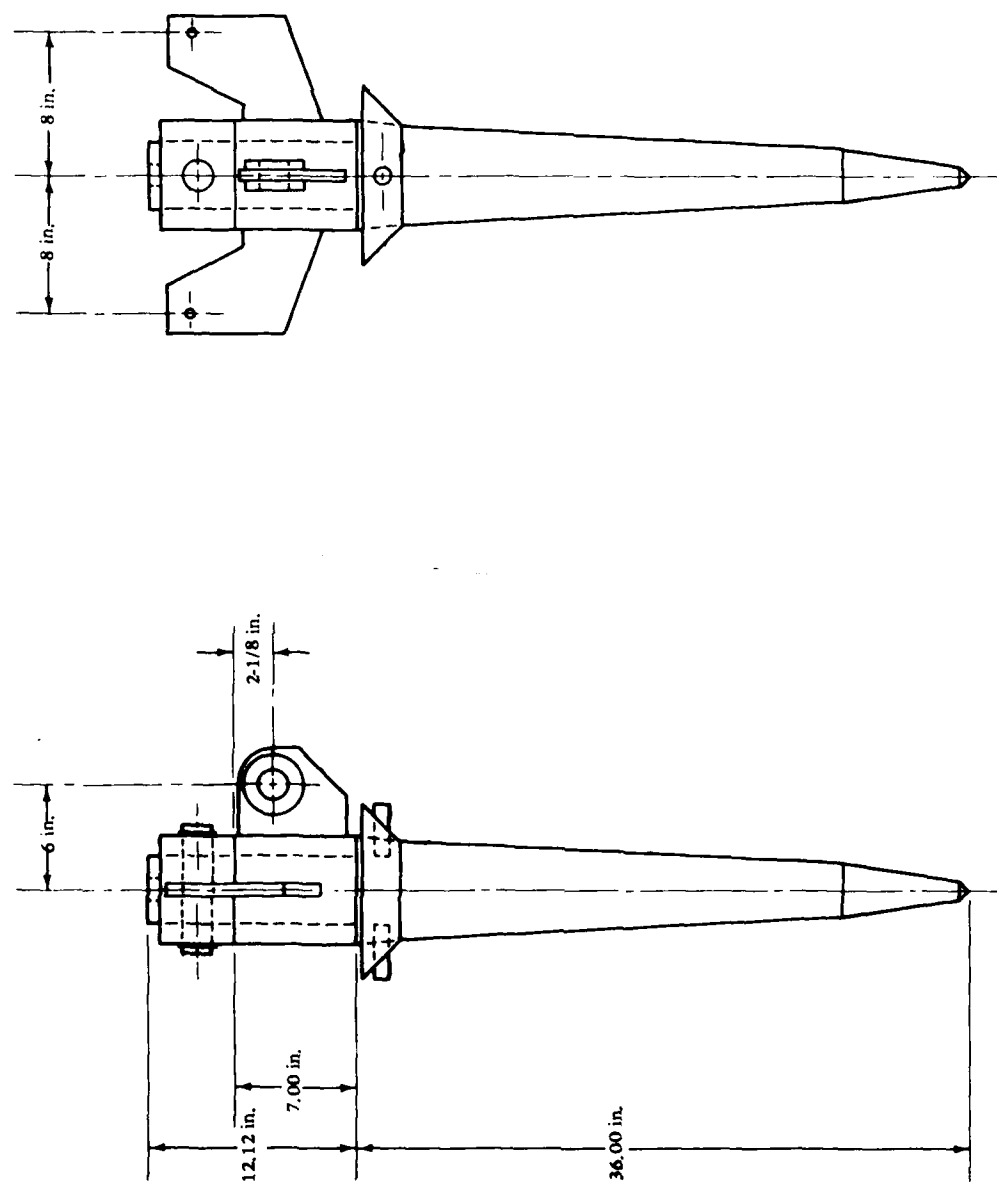


Figure 27. C.F.I. 20K embedment anchor experimental rock fluke.

DISTRIBUTION LIST

AFB CESCH, Wright-Patterson; HQ Tactical Air Cmd/DEMM (Schmidt) Langley, VA; MAC/DET (Col. P. Thompson) Scott, IL; Stinfo Library, Offutt NE
ARCTICSUBLAB Code 54, San Diego, CA
ARMY BMDSC-RE (H. McClellan) Huntsville AL
ARMY COASTAL ENGR RSCH CEN Fort Belvoir VA; R. Jachowski, Fort Belvoir VA
ARMY COE Philadelphia Dist. (LIBRARY) Philadelphia, PA
ARMY CORPS OF ENGINEERS MRD-Eng. Div., Omaha NE; Seattle Dist. Library, Seattle WA
ARMY CRREL A. Kovacs, Hanover NH
ARMY ENG WATERWAYS EXP STA Library, Vicksburg MS
ARMY ENGR DIST. Library, Portland OR
ARMY ENVIRON. HYGIENE AGCY HSE-EW Water Qual Eng Div Aberdeen Prov Grnd MD
ARMY MATERIALS & MECHANICS RESEARCH CENTER Dr. Lenoe, Watertown MA
ARMY MOBIL EQUIP R&D COM Mr. Cevasco, Fort Belvoir MD
ARMY TRANSPORTATION SCHOOL Code ATSPD CD-TE Fort Eustis, VA
ASST SECRETARY OF THE NAVY Spec. Assist Energy (Leonard), Washington, DC; Spec. Assist Submarines, Washington DC
CINCLANT Civil Engr. Supp. Plans. Ofcr Norfolk, VA
CINCPAC Fac Engrng Div (J44) Makalapa, HI
CNO Code NOP-964, Washington DC; Code OP 323, Washington DC; Code OP-413 Wash, DC; Code OPNAV 09B24 (H); Code OPNAV 22, Wash DC; Code OPNAV 23, Wash DC; OP987J (J. Boosman), Pentagon
COMCBPAC Operations Off, Makalapa HI
COMFLEACT, OKINAWA PWO, Kadena, Okinawa
COMNAVBEACHPHIBREFTRAGRU ONE San Diego CA
COMNAVMARIANAS Code N4, Guam
COMOCEANSYSPAC SCE, Pearl Harbor HI
COMSUBDEVGRUONE Operations Offr, San Diego, CA
DEFENSE INTELLIGENCE AGENCY DB-4C1 Washington DC
DLSIE Army Logistics Mgt Center, Fort Lee, VA
DNA STTL, Washington DC
DTIC Defense Technical Info Ctr/Alexandria, VA
DTNSRDC Code 4111 (R. Gierich), Bethesda MD
FMFLANT CEC Offr, Norfolk VA
HCU ONE CO, Bishops Point, HI
MARINE CORPS BASE PWO Camp Lejeune NC; PWO, Camp S. D. Butler, Kawasaki Japan
MCAS Facil. Engr. Div. Cherry Point NC; Code S4, Quantico VA
MCDEC NSAP REP, Quantico VA; P&S Div Quantico VA
MILITARY SEALIFT COMMAND Washington DC
NAF PWO Sigonella Sicily; PWO, Atsugi Japan
NALF OINC, San Diego, CA
NARF Equipment Engineering Division (Code 61000), Pensacola, FL
NAS Code 18700, Brunswick ME; Dir. Util. Div., Bermuda; ENS Buchholz, Pensacola, FL; PWD Maint. Div., New Orleans, Belle Chasse LA; PWD, Willow Grove PA; PWO Belle Chasse, LA; PWO Key West FL; PWO Whiting Fld, Milton FL; PWO, Glenview IL; SCE Norfolk, VA; SCE, Barbers Point HI
NAVACT PWO, London UK
NAVAEROSPREGMEDCEN SCE, Pensacola FL
NAVCOASTSYSSEN Code 772 (C B Koesy) Panama City FL
NAVCOASTSYSTCTR CO, Panama City FL; Code 715 (J Quirk) Panama City, FL; Code 715 (J. Mittleman) Panama City, FL; Library Panama City, FL
NAVCOMMAREAMSTRSTA PWO, Norfolk VA; SCE Unit 1 Naples Italy
NAVCOMMSTA Code 401 Nea Makri, Greece; PWO, Exmouth, Australia
NAVEDTRAPRODEVSEN Technical Library, Pensacola, FL
NAVELEXSYSCOM Code PME-124-61, Washington DC
NAVENVIRHLTHCEN CO, NAVSTA Norfolk, VA
NAVEODFAC Code 605, Indian Head MD

NAVFAC PWO, Centerville Bch, Ferndale CA
NAVFAC PWO, Lewes DE
NAVFACENGCOM Code 043 Alexandria, VA; Code 044 Alexandria, VA; Code 0453 (D. Potter) Alexandria, VA; Code 0454B Alexandria, Va; Code 04B3 Alexandria, VA; Code 04A1 Alexandria, VA; Code 100 Alexandria, VA; Code 1002B (J. Leimanns) Alexandria, VA; Code 1113 (M. Carr) Alexandria, VA; Code 1113 (T. Stevens) Alexandria, VA; Morrison Yap, Caroline Is.
NAVFACENGCOM - CHES DIV. Code 407 (D Scheesle) Washington, DC; Code 405 Wash, DC; FPO-1 (Kurtz) Washington, DC; FPO-1C (Spencer), Washington, DC; FPO-1 Wash, DC
NAVFACENGCOM - LANT DIV. Code 10A, Norfolk VA; Eur. BR Deputy Dir, Naples Italy; European Branch, New York; RDT&ELO 102, Norfolk VA
NAVFACENGCOM - NORTH DIV. (Boretsky) Philadelphia, PA; CO; Code 09P (LCDR A.J. Stewart); Code 1028, RDT&ELO, Philadelphia PA; Design Div. (R. Masino), Philadelphia PA; ROICC, Contracts, Crane IN
NAVFACENGCOM - PAC DIV. Code 2011 Pearl Harbor, HI; Code 402, RDT&E, Pearl Harbor HI; Commander, Pearl Harbor, HI
NAVFACENGCOM - SOUTH DIV. Code 90, RDT&ELO, Charleston SC
NAVFACENGCOM - WEST DIV. AROICC, Contracts, Twentynine Palms CA; Code 04B San Bruno, CA; O9P/20 San Bruno, CA; RDT&ELO Code 2011 San Bruno, CA
NAVFACENGCOM CONTRACT AROICC, Point Mugu CA; Eng Div dir, Southwest Pac, Manila, PI; OICC, Southwest Pac, Manila, PI; ROICC AF Guam; ROICC, Diego Garcia Island; ROICC, Keflavik, Iceland; ROICC, Pacific, San Bruno CA
NAVFORCARIB Commander (N42), Puerto Rico
NAVNUPWRU MUSE DET Code NPU-30 Port Hueneme, CA
NAVOCEANO Library Bay St. Louis, MS
NAVOCEANSYSCEN Code 41, San Diego, CA; Code 4473 Bayside Library, San Diego, CA; Code 52 (H. Talkington) San Diego CA; Code 5204 (J. Stachiw), San Diego, CA; Code 5214 (H. Wheeler), San Diego CA; Code 5221 (R.Jones) San Diego Ca; Code 5311 San Diego, CA; Tech. Library, Code 447
NAVPETRES Director, Washington DC
NAVPGSCOL D. Leipper, Monterey CA; E. Thornton, Monterey CA
NAVPHIBASE CO, ACB 2 Norfolk, VA; Code S3T, Norfolk VA; Dir. Amphib. Warfare Brd Staff, Norfolk, VA; Harbor Clearance Unit Two, Little Creek, VA
NAVREGMEDCEN Chief of Police, Camp Pendleton CA; SCE (D. Kaye)
NAVSEASYSCOM Code SEA OOC Washington, DC
NAVSECGRUACT PWO, Adak AK
NAVSHIPREPFAC Library, Guam; SCE Subic Bay
NAVSHIPYD; Code 202.4. Long Beach CA; Code 380, Portsmouth, VA; Code 440 Portsmouth NH; Code 440, Puget Sound, Bremerton WA; Salvage Supt, Phila., PA; Tech Library, Vallejo, CA
NAVSTA CO Naval Station, Mayport FL; CO Roosevelt Roads P.R. Puerto Rico; Code 4, 12 Marine Corps Dist, Treasure Is., San Francisco CA; Engr. Dir., Rota Spain; Long Beach, CA; PWD (LTJG.P.M. Motolenich), Puerto Rico; PWO Midway Island; PWO, Keflavik Iceland; PWO, Mayport FL; SCE, Guam; SCE, Subic Bay, R.P.; Security Offr, San Francisco, CA
NAVSUPPACT LTJG McGarrah, SEC, Vallejo, CA
NAVSURFWPNEN PWO, White Oak, Silver Spring, MD
NAVTECHTRACEN SCE, Pensacola FL
NAVWPNCEN Code 2636 (W. Bonner), China Lake CA
NAVWPNSTA Code 092, Colts Neck NJ
NAVWPNSTA PW Office (Code 09C1) Yorktown, VA
NAVWPNSTA PWO, Seal Beach CA
NAVWPNSUPPCEN Code 09 Crane IN
NCBU 405 OIC, San Diego, CA
NCBC Code 10 Davisville, RI; Code 155, Port Hueneme CA; Code 156, Port Hueneme, CA
NCR 20, Commander
NMCB 5, Operations Dept.; 74, CO; Forty, CO; THREE, Operations Off.
NORDA Code 410 Bay St. Louis, MS; Code 440 (Ocean Rsch Off) Bay St. Louis MS
NRL Code 5800 Washington, DC; Code 8441 (R.A. Skop), Washington DC; Code 5843 (F. Rosenthal) Washington, DC
NSC Code 54.1 (Wynne), Norfolk VA

NSD SCE, Subic Bay, R.P.

NUSC Code 131 New London, CT; Code EA123 (R.S. Munn), New London CT; Code 332, B-80 (J. Wilcox)
New London, CT; Code TA131 (G. De la Cruz), New London CT

OCEANAV Mangmt Info Div., Arlington VA

OCEANSYSLANT LT A.R. Giancola, Norfolk VA

ONR Code 485 (Silva) Arlington, VA; Central Regional Office, Boston, MA; Code 481, Bay St. Louis, MS;
Code 700F Arlington VA; Dr. A. Laufer, Pasadena CA

PHIBCB 1 P&E, Coronado, CA

PMTTC Code 3331 (S. Opatowsky) Point Mugu, CA; EOD Mobile Unit, Point Mugu, CA; Pat. Counsel, Point
Mugu CA

PWC CO Norfolk, VA; CO, (Code 10), Oakland, CA; CO, Great Lakes IL; Code 10, Great Lakes, IL; Code
120, Oakland CA; Code 120C, (Library) San Diego, CA; Code 128, Guam; Code 154, Great Lakes, IL;
Code 200, Great Lakes IL; Code 220.1, Norfolk VA; Code 30C, San Diego, CA; Code 400, Great Lakes,
IL; Code 400, Pearl Harbor, HI; Code 400, San Diego, CA; Code 420, Great Lakes, IL; Code 420,
Oakland, CA; Code 505A (H. Wheeler); Code 700, Great Lakes, IL; Code 700, San Diego, CA

UCT TWO OIC, Norfolk, VA; OIC, Port Hueneme CA

US NAVAL FORCES Korea (ENJ-P&O)

USCG G-ECV (C E Smith) Washington, DC

USNA Civil Engr Dept (R. Erchyl) Annapolis MD; Ocean Sys. Eng Dept (Dr. Monney) Annapolis, MD; PWD
Engr. Div. (C. Bradford) Annapolis MD